HHS Public Access

Author manuscript

Arch Biochem Biophys. Author manuscript; available in PMC 2015 December 11.

Published in final edited form as:

Arch Biochem Biophys. 2012 January 1; 517(1): 53–70. doi:10.1016/j.abb.2011.11.005.

Identification of agents that reduce renal hypoxia-reoxygenation injury using cell-based screening: purine nucleosides are alternative energy sources in LLC-PK1 cells during hypoxia

Petra Szoleczky[1,2], **Katalin Módis**[1,2], **Nóra Nagy**[1], **Zoltán Dóri Tóth**[1], **Douglas DeWitt**[2], **Csaba Szabó**[1,2], and **Domokos Gerő**[1,2,*]

[1]CellScreen Applied Research Center, Semmelweis University Medical School, Budapest, Hungary

[2]Department of Anesthesiology, The University of Texas Medical Branch, Galveston, TX 77555, USA, Semmelweis University Medical School, University of Texas Medical Branch

Abstract

Acute tubular necrosis is a clinical problem that lacks specific therapy and is characterized by high mortality rate. The ischemic renal injury affects the proximal tubule cells causing dysfunction and cell death after severe hypoperfusion. We utilized a cell-based screening approach in a hypoxia-reoxygenation model of tubular injury to search for cytoprotective action using a library of pharmacologically active compounds. Oxygen-glucose deprivation (OGD) induced ATP depletion, suppressed aerobic and anaerobic metabolism, increased the permeability of the monolayer, caused poly(ADP-ribose) polymerase cleavage and caspase-dependent cell death. The only compound that proved cytoprotective either applied prior to the hypoxia induction or during the reoxygenation was adenosine. The protective effect of adenosine required the coordinated actions of adenosine deaminase and adenosine kinase, but did not requisite the purine receptors. Adenosine and inosine better preserved the cellular ATP content during ischemia than equimolar amount of glucose, and accelerated the restoration of the cellular ATP pool following the OGD. Our results suggest that radical changes occur in the cellular metabolism to respond to the energy demand during and following hypoxia, which include the use of nucleosides as an essential energy source. Thus purine nucleoside supplementation holds promise in the treatment of acute renal failure.

Keywords

acute renal failure; acute tubular necrosis; cell-based screening; adenosine; inosine; ischemic kidney injury

[*]**Address for correspondence:** Domokos Gero M.D., Department of Anesthesiology, The University of Texas Medical Branch, 601 Harborside Drive, Building 21, Room 3.202I, Galveston, TX 77555-1102, Phone: 409 747 5383, FAX 409 772 6409, Cell: 409 457 8419, gerodomokos@yahoo.com.

Introduction

Acute tubular necrosis (ATN), defined as acute renal failure (ARF) due to ischemic or toxic renal injury, is a clinical syndrome that commonly occurs in critically ill patients in the intensive care units and is often associated with various co-morbidities in the elderly. During the last decades a considerable amount of research has been devoted to elucidating the pathophysiology of ATN with the ultimate goal to facilitate the development of therapeutic interventions that either prevent ARF, ameliorate the severity of tubular injury following an acute renal insult, or accelerate the recovery of established ATN. Despite the major advances in our understanding of pathogenic events in ischemiareperfusion injuries and that of ATN, neither the clinical outcomes nor the therapeutic approaches changed considerably over the past decades. This is also illustrated by the fact that, while the therapeutic arsenal noticeably expanded in the treatment of ischemiareperfusion based illnesses of other organs, saline-induced intravascular volume expansion remained the basis of ARF therapy supplemented with renal replacement therapy. A recent metaanalysis showed that even some of the traditionally employed treatment modalities like renal vasodilators and diuretics lacked any beneficial effect [1, 2].

The “imperfect” experimental models that do not accurately simulate the clinical disease were generally accounted for the failure to translate basic, laboratory-derived, mechanistic insights into clinical practice and led to the development of more complex models with little success [3, 4]. The strategy to transfer successful therapeutic approaches of similar, ischemia-reperfusion diseases of other organs equally failed in ARF, including those targeting the renal vasculature suggesting an inherent difference in the mechanism of ATN. From recent advances only the antioxidant N-acetylcystein holds promise for reducing the oxidative stress in the kidney, especially in radiocontrast injury [1, 5].

The critical area of ischemic renal injury is the proximal tubule. According to widely accepted beliefs the high energy requiring transport function of this segment renders the epithelial cells within this part vulnerable to ischemic kidney injury, since the transport needs can rapidly deplete the cellular ATP content. Also, the renal microcirculation (namely the peritubular capillaries coming from the efferent arterioles) supplying these segments is implicated in the high susceptibility to injury, as the provider of insufficient blood flow during the reperfusion due to microcirculatory changes [6]. However, on a simply theoretical basis, this view is dubious since the transport demand rapidly decreases with the reduction of blood flow and filtration rate. Also, the high energy consumption is reflected in dense capillary structures along the tubules that may provide superior blood supply compared to what most cells receive in the body. Furthermore, the tubular epithelium benefits from glucose and other energy source supplies from the tubular side, and possesses high-affinity transport systems to take up these compounds. The lack of sufficient energy supply during the reperfusion is further opposed by the fact of glucosuria in ARF [7] confirming the presence of adequate glucose supply via the filtrate. These notions strongly support the idea that the proximal tubule epithelial cells, in fact, may enjoy better conditions than most other cells of the kidney during and after an ischemic period, suggesting that the acute tubular necrosis is rather based on unique and intrinsic functional characteristics of these cells than their cellular environment.

This scenario prompted us to reconsider some of the widely accepted beliefs in ARF and focus our studies on the tubular epithelial cells. We chose a cellular model of tubular injury that employs true hypoxia and performed a systematic search for compounds that protect against the injury. The use of cell-based screening approach with the evaluation of the overall protection against fatal injury permitted a variety of actions exerted by the wide array of molecules by interacting with multiple targets simultaneously without the need to act on any of the currently known targets in renal injury [8, 9]. Also, this methodology allowed a direct comparison of the efficacy of the tested compounds on the eventual outcome, thus provided us with an estimate of the contribution of various pathways in the development of tubular injury.

Material and methods

Reagents

A library of 1280 pharmacologically active compounds (LOPAC) was obtained from Sigma-Aldrich (St Louis, MO). The library includes drug-like molecules in the field of cell signaling and neuroscience. The compounds are dissolved at 10 mM in dimethylsulfoxide (DMSO) and dilutions were made either in DMSO or in phosphate-buffered saline (PBS, pH 7.4) to obtain 0.5% DMSO in the assay volume. Adenosine (ADE), inosine (INO), glucose, PJ34, 8-cyclopentyl-1,3-dipropylxanthine, 8-(3-chlorostyryl) caffeine, alloxazine, MRS 1523, erytro-9-(2-hydroxy-3-nonyl)adenine hydrochloride (EHNA), [4-amino-5-(3-bromophenyl)-7-(6-morpholino-pyridin-3-yl)pyrido(2,3-d)pyrimidine (ABT702), oligomycin, carbonyl cyanide *p*-trifluoromethoxyphenylhydrazone (FCCP), antimycin A were purchased from Sigma-Aldrich (St Louis, MO), necrostatin-1 (NEC) from Calbiochem (EMD BioSciences, San Diego, CA), carbobenzoxy-valyl-alanyl-aspartyl-[O-methyl]-fluoromethylketone (Z-VAD-fmk) from Promega (Madison, WI). All compounds were dissolved in DMSO except for adenosine, inosine and glucose which were dissolved in culture medium.

Cell culture

LLC-PK1 porcine kidney proximal tubular cells were obtained from American Type Culture Collection (Manassas, VA) and maintained in Dulbecco's modified Eagle's medium (DMEM) (Hyclone, Logan, UT)) containing 1g/l glucose supplemented with 10% fetal bovine serum (PAA Laboratories, Dartmouth, MA), 4mM glutamine and 100 IU/ml penicillin and 100 μg/ml streptomycin (Invitrogen, Carlsbad, CA). 3,000 cells/well were plated into 96-well tissue culture plates and 100,000 cells were plated into 60-mm culture dishes and cultured for 4 days at 37 °C in 5% CO_2 atmosphere.

In vitro model of acute tubular necrosis

Culture medium was replaced with DMEM containing no glucose prior to the induction of hypoxia. In the pretreatment assay the drugs were added at 50 μM concentration in 5% of the culture volume (final concentration of DMSO was 0.5%). Culture plates were placed in gas-tight incubation chambers (Billups-Rothenberg Inc., Del Mar, CA) and the chamber atmosphere was replaced by flushing the chamber with 95% N_2/5% CO_2 mixture at 25 L/min flow rate for 5 min. The hypoxia was maintained by clamping and incubating the

chambers for 20 hours (or for the indicated period) at 37 °C. All assay plates subjected to hypoxia included vehicle-treated control wells with glucose-free medium (OGD) or medium containing 5mM glucose (CTL). After hypoxia, glucose and serum concentration was restored by supplementing the culture medium with glucose and FBS and the cells were incubated for 24 hours at 37 °C at 5% CO_2 atmosphere. In the post-treatment assay the drugs were added immediately after the hypoxia at 50 μM final concentration in 5% of the culture volume.

Viability assays

MTT viability assay—The MTT assay was performed as previously described with slight modification [10]. Briefly, cells were dissociated with 0.05 mM EDTA (at a final concentration of 2.5 μM) at 37 °C for 15 min at 5% CO_2 atmosphere, then 1/10 volume FBS containing 3-(4,5-dimethyl-2-thiazolyl)-2,5-diphenyl-2H-tetrazolium bromide (MTT, Calbiochem, EMD BioSciences, San Diego, CA) was added in 1/10 volume to reach final concentration of 0.5 mg/mL, and the cells were incubated for 3 hours at 37°C at 5% CO_2 atmosphere. The converted formazan dye was detected at 570 nm with background measurement at 690 nm and viable cell count was calculated using a calibration curve created with serial dilutions of LLC-PK1 cells.

Alamar blue cell viability assay—Following the 24 hour long recovery period, the cells were pretreated with EDTA at a final concentration of 2.5 μM for 15 min at 37 °C to allow complete dye uptake. Then FBS was added to the cells to neutralize EDTA and Alamar Blue (resazurin, 7-hydroxy-3H-phenoxazin-3-one-10-oxide) at a final concentration of 10 mg/mL. The cells were incubated for 3 hours at 37°C at 5% CO_2 atmosphere and fluorescence was measured on Synergy2 reader (Ex/Em: 530/590 nm) (Biotek, Winooski, VT, USA). The viability was calculated using dilution series of LLC-PK1 cells for calibration.

Biochemical assays

Lactate dehydrogenase (LDH) assay—LDH release was measured as previously described [10]. Cell culture supernatant (30 μl) was mixed with 100 μl freshly prepared LDH assay reagent and the changes in absorbance were read kinetically. LDH release values are shown as Vmax (mOD/min) or percent values compared to the OGD group.

Measurement of cellular ATP content—LLC-PK1 cultures were exposed to 20 hours of combined oxygen-glucose deprivation and 0-8-24 hours of reoxygenation in 96-well plates. ATP concentration was determined by the commercially available CellTiter-Glo® Luminescent Cell Viability Assay (Promega, Madion, WI) that is based on ATP requiring luciferin-oxyluciferin conversion mediated by a thermostable luciferase generating a stable “glow-type” luminescent signal. The cells were lysed in 100 μL of CellTiter-Glo reagent according to the manufacturer's recommendations and the luminescent signal was recorded for 1s on a high sensitivity luminometer (Synergy 2, Biotek,Winooski, VT, USA).

Measurement of caspase-3 activity using a fluorescent substrate—LLC-PK1 cultures were exposed to 20 hours of combined oxygen-glucose deprivation in 96-well

plates. Following 0-1-3-8-24 h reoxygenation, cells were lysed and caspase-3 activity was measured by CaspACE™ Fluoremetric Assay System (Promega, Madison, WI) according to the manufacturer's recommendations. Cell lysates were mixed with caspase-3 specific fluorescence substrate, fluoro-chrome-7-amino-4-methyl-coumarin (Ac-DEVD-AMC). Cleaved generated free AMC that was detected using fluorescence reader (Ex/Em: 360/460nm). The fluorescence signal of free AMC, which is proportional to caspase-3 activity present in the sample, is shown as relative fluorescence units (RFU).

Detection of active Caspase-3 and PARP cleavage by western blotting—Cells were lysed in 400 μl denaturing loading buffer (20 mM Tris, 2% SDS, 10% glycerol, 6 M urea, 100 μg/ml bromophenol blue, 200 mM ß-mercaptoethanol), sonicated and boiled. Lysates (10 μl) were resolved on 4-12% NuPage Bis-Tris acrylamide gels (Invitrogen, Carlsbad, CA) and transferred to nitrocellulose. Membranes were blocked in 10% non-fat dried milk and probed overnight with anti-caspase-3 antibody (1:100, Chemicon, Temecula, CA) or anti-PARP antibody (1:2,000, Cell Signaling, Boston, MA). Anti-rabbit-horseradish peroxidase conjugate (HRP, 1:2,000, Cell Signaling) and Pierce enhanced chemiluminescent substrate (Pierce ECL, Thermo Fisher Scientific Inc., USA) were used to detect the chemiluminescent signal in a CCD-camera based detection system (GBox, Syngene USA, Frederick, MD). To normalize signals, membranes were stripped and reprobed with an antibody against α-tubulin as previously described [10] The active caspase-3 signal at 17 kD, full length PARP-1 at 120 kDa and the chemiluminescent signal at ~50 kDa for tubulin were quantitated with Genetools analysis software.

Functional assays

Trypan blue exclusion test—LLC-PK1 cells were exposed to OGD or glucose deprivation only for 20 hours, then trypan blue dye was added to the cells at the final concentration of 0.01% for 10 min. Excess dye was aspirated and the cells were visualized using a phase contrast microscope (Nikon TS-100F, Nikon Instruments, Inc.).

Permeability measurement—The apical membrane of LLC-PK1 cells is nonpermeable to 3-(4,5-dimethyl-2-thiazolyl)-2,5-diphenyl-2H-tetrazolium bromide (MTT, Calbiochem, EMD BioSciences, San Diego, CA), thus the confluent monolayer of the cells excludes the dye, while the disruption of the monolayer allows dye uptake through the basolateral surface. LLC-PK1 cells underwent 20-hour-long OGD, then MTT was added at a final concentration of 0.5 mg/mL, and the cells were incubated for 3 hours at 37°C at 5% CO_2 atmosphere. The formazan dye taken up and reduced by the cells was dissolved in isopropanol. The absorbance was measured at 570 nm with background measurement at 690 nm. The increase in the amount of dye uptake is expressed as fold increase compared to control cells deprived of glucose only.

Bioenergetic measurements using the Seahorse analyzer—An XF24 Analyzer (Seahorse Biosciences, Billerica, MA) was used to measure metabolic changes in LLCPK1 cells. The XF24 creates a transient 7 μl chamber in specialized microplates that allows real-time measurement of oxygen and proton concentration changes via specific fluorescent dyes and calculates OCR (oxygen consumption rate) and ECAR (extracellular acidification rate),

measures of mitochondrial respiration and glycolytic activity. The proton production rate is similarly denotes the cellular acid production but in pMol/min, while ECAR is expressed in pH/min. The OCR and ECAR values represent the metabolism of cells, but may also reflect the number of viable cells [11]. LLC-PK1 cells underwent OGD as described above and were either used immediately for metabolic analysis or a 24 hour-long recovery period was allowed prior to metabolic measurements. For all bioenergetic measurements, the culture medium was changed to unbuffered DMEM (pH 7.4) containing 5 mM glucose, 2 mM L-glutamine and 1 mM sodium pyruvate. After determining the basal OCR and ECAR values, oligomycin, FCCP and antimycin A were injected through the ports of the Seahorse Flux Pak cartridge to reach final concentrations of 1 μg/ml, 0.3 μM and 2 μg/ml, respectively, to determine the amount of oxygen consumption linked to ATP production, the level of non-ATP-linked oxygen consumption (proton leak) as well as the maximal respiration capacity and the non-mitochondrial oxygen consumption.

Statistical analysis

Data are shown as mean ± SEM values. One-way analysis of variance (ANOVA) was used to detect differences between groups. Post hoc comparisons were made using Tukey's test. A value of $p < 0.05$ was considered statistically significant. All statistical calculations were performed using Prism 4 analysis software (GraphPad Software, Inc., La Jolla, CA).

Results

Oxygen-glucose deprivation induces a gradual viability decrease in LLC-PK1 cells

A cellular model of ischemic acute tubular necrosis was created by deprivation of oxygen and glucose followed by a recovery period to mimic the reperfusion injury (Fig. 1A). When LLC-PK1 cells were exposed to hypoxia (oxygen deprivation) in a medium containing 5 mM glucose for up to 20 hours, we did not detect a decrease in viability measured after a 24-hour-long reoxygenation (recovery) period. Similarly, 8 to 20 hours of glucose deprivation (GD) resulted in no change in the viable cell counts as measured after the 1-day long recovery. However, the combined deprivation of both oxygen and glucose (OGD) caused a proportional decrease in the viability. An 8-hour long OGD was without effect, but an OGD of 12, 16, 18 or 20 hours reduced the viability by 15%, 30%, 65% or 80%, respectively (Fig. 1B).

OGD induced the loss of trypan blue excluding ability of the cells. While oxygen deprivation (OD) alone had no effect on trypan blue exclusion (Fig. 2A), near 100% of the cells subjected to OGD stained with trypan blue (Fig. 2B). The inability to exclude or actively remove trypan blue from the cells may reflect the loss of barrier function of the cell membrane or the lack of energy to properly function the active machinery that helps exclude and/or remove the dye.

The apical membrane is impermeable to MTT, thus the confluent LLC-PK1 cells do not take up and retain MTT without the disruption of barrier function of the monolayer. Glucose deprivation induced a low, but measurable MTT uptake in the cells, and OGD induced a 3-fold increase in the amount of MTT taken up by the cells or transferred to the basolateral

side of the monolayer (Fig. 2C), which either reflects the increased permeability of the apical membrane, or increased paracellular transport and the loosening of the intercellular tight junctions or dislocation of transporters and opportunity for inappropriate transcellular transport, and overall a decrease of the barrier function and increased permeability of the monolayer.

OGD induced a severe reduction in the cellular ATP content of the cells: a 20-hour-long exposure reduced the ATP content below 5% of control values that increased at least 4-fold reaching approximately 20% of the controls during the 24-hour-long recovery period (Fig. 2D). OGD did not induce an immediate increase in the LDH release form the cells: there was no detectable difference between the LDH release of the cells subjected to OGD and control cells following the hypoxia (Fig. 2E). However, during the recovery period the LDH release significantly increased in the OGD group, suggesting that the above described partly reversible alterations measured immediately after the hypoxia rather reflect cellular dysfunction as a result of ATP depletion than cell death. Definitive cell death did not occur during the hypoxia, but it was detectable during the recovery period.

Apoptotic and proteolytic pathways are implicated in the OGD induced cell death in LLC-PK1 cells

To characterize the mechanism of the late phase cell death after OGD, we tested the effect of compounds that selectively inhibit various forms of cell death. The cells were treated after the hypoxia with caspase inhibitor Z-VAD-fmk, the necroptosis inhibitor necrostatin-1 or the poly(ADP-ribose)polymerase (PARP) inhibitor PJ34. Neither PJ34 nor necrostatin-1 provided protection against the OGD induced cell death (Fig. 3A). On the other hand, inhibition of apoptosis using Z-VAD-fmk resulted in a significant increase in cellular viability. Caspase inhibition induced a two-fold increase in the viability after severe OGD, still the majority of the cells receiving Z-VAD-fmk treatment died eventually. Caspase inhibitor treatment preceding the OGD was similarly effective, but it had no benefit over the post-OGD treatment.

We also studied the time course of caspase activation by Western blotting and using an activity assay. Active caspase-3 was hardly detectable in the samples immediately after the OGD, but appeared within 1 hour of the reoxygenation period and was detectable subsequently for hours (Fig. 3B). Similarly, the caspase activity assay showed increased caspase-3 activity 1 hour following the end of the OGD and the activity further increased in the following hours peaking by 8 hours of the reoxygenation period (Fig. 3C). However, active caspase-3 was not detectable by Western blotting at the end of the 24-hour-long recovery period, and also the caspase activity returned to baseline level by that time.

Caspases cleave various proteins during the apoptotic process, including PARP, a nuclear enzyme associated with necrotic cell death. Caspase cleavage of PARP-1 removes the DNA-binding domain of the protein from its catalytic domain, creating 30 kDa and 89 kDa fragments [12, 13]. We detected a decrease in full length (120 kDa) PARP-1 during the reoxygenation phase: 1 hour following the beginning of the reoxygenation the amount of full length PARP1 significantly decreased, followed by further reduction in PARP-1 level. Full-length PARP-1 was hardly detectable by 8 hours and it completely disappeared at the end of

the 24-hour-long recovery period, whereas there was hardly any change in the expression of the structural protein tubulin (Fig. 3D). The decrease of full-length PARP-1 was associated with an increase of cleavage fragments. The caspase-specific 89 kDa fragment appeared in some of the samples taken immediately after the OGD and reached peak levels by 3 hours of reoxygenation, then started to decline, but remained detectable by the end of the 24-hour-long recovery period.

Other proteases that cleave PARP-1 include calpain, cathepsin B and granzyme B which create 70 kDa, 64 kDa and 50 kDa fragments, respectively [14-16]. The calpain specific 70 kDa fragment was detectable 1 hour following the OGD (but not immediately at the end of the OGD), and was present in all subsequent samples at high levels throughout the reoxygenation period. The cathepsin B specific 64 kDa fragment was detectable at low levels in samples taken 1 hour after the OGD and remained detectable up to 8 hours of the recovery period. The 50 kDa fragment associated with granzyme B mediated cleavage was present in the samples from the end of the hypoxia and remained detectable throughout the 24-hour follow-up. All proteolytic fragments of PARP reached the highest level in the samples taken 3 hours after the beginning of the reoxygenation. The calpain specific fragment was present in the highest amount in all the samples taken after 1 hour of reoxygenation or later.

Adenosine protects against the hypoxia-reoxygenation injury in LLC-PK1 cells

We searched for compounds that ameliorate hypoxia-reoxygenation injury of renal proximal tubule cells in two settings: cells were subjected to 20 hours of OGD followed by a 24 hour-long reoxygenation period with the test compounds either added prior to the OGD induction (pre-OGD screen) or immediately after the onset of the reoxygenation (post-OGD screen) (Fig. 4A). The majority of the compounds had negligible effect on the OGD induced injury (Fig. 4B). The compounds exerting the highest protective activity in the screens are summarized in Table 1. Adenosine was the only compound that showed high activity in both assays. In fact, it was the only compound that increased the viability by more than 40% in the pretreatment screen, and was among the top 10 compounds in the post-OGD screen with 13% increase in the viability. The high activity of adenosine in our screens and the fact that adenosine is known to be released from the cells during ischemia or inflammation and may reach similar local concentration urged us to search for potentiators of adenosine. We performed two additional screens in which the same compound library was screened with 30 μM adenosine pretreatment either with pre-OGD or post-OGD addition of the test compounds. In these screens the highest-ranking compounds included only two of the drugs that emerged as protective in the previous screens: adenosine in the pre-OGD and L-aspartic acid in the post-OGD regimen. Adenosine was among the most potent compounds in the pre-OGD combination screen, showing that higher concentration of adenosine has further benefit and it affects the cell survival more than most other treatments. PARP inhibitor 4-amino-1,8-naphthalimide exerted protection against the OGD induced cell death in combination with adenosine, and some other PARP inhibitors (PJ34, 1,5-isoquinolinediol) showed similar but more modest protective effect (Table S1). Also, the dompaminergic R(+)-6-bromo-APB, which we have shown to possess PARP inhibitory effect [10], increased the cell survival.

Adenosine and inosine increase the survival after OGD with similar efficacy

We also inosine, adenosine's metabolite, that has less cardiovascular activity but retains most of adenosine's anti-inflammatory potential [17]. Both adenosine and inosine increased cell survival in a dose dependent manner in our model. The protective effect of these purine nucleosides was similar to that of glucose (Fig. 5A and B). Adenosine exerted significant cytoprotection at 30 μM as measured with the MTT assay, while inosine and glucose were less effective, though both adenosine and glucose decreased the LDH release already at 10 μM (Fig. 5C). 100 μM of any of the three compounds (adenosine, inosine or glucose) induced a significant viability increase and significant reduction of LDH release. All three compounds mostly reverted the hypoxic injury at 300 μM. The MTT assay indicated complete reversal of the injury at 300 μM for all three compounds, while the alamar blue assay showed only 90% restoration for adenosine and inosine and approximately 75% functional recovery after glucose treatment. The LDH release was also lower in the purine-treated wells than in the wells receiving glucose treatment in the 100-1000 μM range.

OGD induced caspase activation during the reoxygenation phase that was significantly reduced by inosine pretreatment (Fig. 5D). OGD induced a severe reduction of full length PARP, 8 hours after the beginning of reoxygenation only 10% of intact PARP remained detectable, while adenosine pretreatment protected PARP and restored it to 60% of the control level (Fig. 5E and F). In agreement with the preservation of full-length PARP we also detected reduction in the various cleavage products (data not shown).

The cytoprotective effect of purine nucleosides requires intracellular metabolism

Adenosine was shown to protect against ischemia-reperfusion injury and inflammation and the various adenosine receptors were implicated in the protective action suggesting that these receptors are essential in the protective function of adenosine in hypoxiareoxygenation based injuries. We tested whether blockade of the adenosine receptors prevents the protective action of adenosine or inosine against the OGD induced cell death in LLC-PK1 cells. Treating the cells with A_1 receptor antagonist CDPX or A_{2A} receptor antagonist 8-(3-chlorostyryl)caffeine or A_{2B} receptor antagonist alloxazine or with A_3 receptor antagonist MRS 1523 did not reduce the viability increase attained by adenosine or inosine (Fig. 6A and B). Neither affected the adenosine receptor antagonists the adenosine or inosine induced decrease of the LDH release in LLC-PK1 cells exposed to hypoxia (Fig. 6C and D). These data indicate that receptor-independent actions are involved in the protective actions of adenosine and inosine in LLC-PK1 cells.

The similar efficacy of inosine and adenosine suggested that the cells convert adenosine to inosine and inosine is responsible eventually for the protective effect. We blocked adenosine deaminase (ADA), the enzyme that converts adenosine to inosine within the cells, with pharmacological inhibitor EHNA [18, 19]. As expected, EHNA did not reduce the protective effect of inosine or glucose but significantly decreased the viability of the adenosine treated cells subjected to OGD and also significantly increased the LDH release from the cells (Fig. 7A and B). However, ADA inhibition did not abolish the adenosine-mediated protection completely. Adenosine is phosphorylated by adenosine kinase (AK) within the cells to produce AMP, which is an ATP consuming process, thus it can be harmful under ATP

depleting conditions. The inhibition of AK with ABT 702 resulted in a mild increase in viability in the absence of exogenous adenosine, supporting that this enzyme may cause more harm under severely restrictive conditions (Table S1). However, ABT 702 also reduced the adenosine and inosine induced viability increase after OGD in LLC-PK1 cells. The AK and ADA inhibition resulted in comparable viability decrease in the adenosine treated cells, and similar increase in the LDH release. Also AK inhibition similarly affected the viability and LDH release in both the adenosine and the inosine treated cells, whereas it had no significant effect on the glucose treated cells. The simultaneous inhibition of ADA and AK completely abolished the protective effect of adenosine and inosine. Also, the combination of EHNA and ABT702 significantly reduced the glucose mediated viability increase and also increased the LDH release.

Adenosine and inosine accelerate the post-hypoxic recovery

ATP depletion plays a crucial role in the pathogenesis of hypoxia-reoxygenation injury and the requirement of AK activity in the protection mediated by adenosine and inosine suggested that these purine nucleosides act via promoting ATP synthesis and preserving the ATP content during hypoxia. We measured the ATP content of the cells receiving 300 μM adenosine, inosine or glucose treatment prior to the OGD. OGD induced 60% decrease in the viability and the compound treatments fully restored the viability of the cells according to the viability assay. Both adenosine and inosine significantly increased the cellular ATP content as measured immediately after the OGD. The ATP content dropped to 5% in LLC-PK1 cells subjected to hypoxia and both purine nucleosides elevated the ATP content to 20%, while the presence of glucose in equal amounts increased the ATP content to 10% only (Fig. 8A). During the recovery period, ATP concentration increased gradually in all groups. The ATP content of the cells subjected to OGD reached 10% and 20% after 8 and 24 hours of reoxygenation, respectively. In the cells exposed to hypoxia in the presence of glucose the ATP content was 30% and 60% after 8 and 24 hours of reoxygenation, while in the cells supplemented with purines the ATP content exceeded 60% by 8 hours and was completely restored by 24 hours. The cellular ATP content decreased severely during the hypoxia, and both glucose and purine pretreatment helped preserving the ATP content to some extent, still this effect seems to be moderate. In the presence of adenosine or inosine LLC-PK1 cells tolerated such severe ATP depletion with full recovery that may induce cell death in other cells. The purines also enhanced the restoration of the ATP content, since they resulted in a steeper increase in the ATP content and they fully replenished the cellular ATP concentration by 24 hours, while glucose supplementation also fully prevented cell death, still resulted in a significantly lower cellular ATP concentration at the end of the 24-hour-long follow-up. We blocked ADA and AKA function during the reoxygenation period to test whether these enzymes also take part in the recovery after hypoxia. Both the post-hypoxic ADA and AK inhibition decreased the ATP content (Fig. 8B), proving the requirement of ADA and AKA function during the reoxygenation period. ADA or AK inhibition after the OGD significantly reduced the ATP content of the adenosine-pretreated cells. Interestingly, EHNA significantly reduced the ATP content of inosine and glucose treated groups, possibly by blocking the utilization of endogenous adenosine via the pentose phosphate pathway. AK inhibition resulted in a more pronounced viability reduction in all treatment groups. The effect of ADA and AK inhibition showed no synergism during the recovery.

Unlike during the hypoxia, ADA inhibition did not further decrease the ATP content compared to the effect of AK blockade but rather showed the opposite effect, a slight tendency to increase the ATP content of the cells. These data strongly suggest that metabolism of endogenous or exogenous adenosine and inosine also assisst ATP production during the post-hypoxic reoxygenation period.

Adenosine and inosine ameliorate the OGD-induced metabolic suppression in LLC-PK1 cells

Adenosine is supposed to be used as a ribose source in place of glucose to maintain ATP generation during hypoxia. Thus we tested whether adenosine pretreatment directly affect the cellular metabolism using the Seahorse metabolic analyzer.

LLC-PK1 cells were subjected to hypoxia with 300 μM adenosine pretreatment and the cellular metabolism was measured immediately following the hypoxia and after a 24-hour-long recovery period. OGD induced very severe reduction in both aerobic and anaerobic metabolism, the oxygen consumption rate (OCR) of the cells was lower than the detection limit of the instrument while the acid production (ECAR), the measure of the anaerobic metabolism, was below 10% of the controls (Fig. 9). (The Seahorse analyzer uses fluorescent detection method to measure changes of partial pressure of oxygen in the assay medium and is unable to reliably detect a drop less than 50 mmHg or OCR values under 30-40 pMoles/min.) Adenosine pretreatment completely preserved the anaerobic metabolism in the cells and resulted in approximately 40% decrease in the oxygen consumption. Anaerobic metabolism is often described with the proton production rate (PPR) that is calculated from the pH changes of the assay medium and it is also expressed in a logarithmic scale as extracellular acidification rate (ECAR) in pH/min. The assay medium acidification is proportional to the CO_2 production as glucose represents the major energy source during the measurement and during glucose metabolism CO_2 is produced in an anaerobic fashion while the protons retrieved from glucose are not released from the cell but proceed to the oxidative phosphorylation. The Seahorse analyzer measures the water production from the retrieved protons as oxygen consumption (OCR). The two parameters (OCR and PPR) are directly proportional if glucose is the only energy source: 1 pMol/min PPR represents 1 pMol/min CO_2 production that also generates 2 pMol/min protons and is able to consume ½ pMol/min O_2 to produce 1 pMol/min H_2O. Therefore the complete glucose breakdown ideally gives OCR values that are one half of PPR, while lower basal OCR values represent incomplete glucose oxidation. We detected OCR:PPR ratios close to 1:2 in the controls representing complete glucose breakdown, while in the adenosine pretreated cells subjected to hypoxia the OCR:PPR ratio was around 1:3 that means a lower rate of mitochondrial proton utilization. The acidification rate of the controls and the adenosine-pretreated cells was comparable showing that adenosine supplementation completely preserved the cellular machinery required for anaerobic glucose metabolism, while it was severely damaged in oxygen-glucose deprived cells. Proton leak is implicated in the mitochondrial damage and it can be measured with the Seahorse analyzer as the difference between the OCR values after oligomycin and antimycin addition. There was no detectable proton leak in the adenosine-pretreated cells after hypoxia, but there was a reduction in the mitochondrial potential (shown by the lower OCR after FCCP addition).

These data suggest that rather the decreased mitochondrial potential (possibly as a result of lower proton production during the OGD) than mitochondrial dysfunction cause the lower basal mitochondrial oxygen consumption and aerobic metabolism after adenosine treatment.

We also tested the metabolic function in the cells subjected to hypoxia 24 hours later when the ATP content of the cells was fully restored in the adenosine-pretreated cells. There was very little improvement in both the aerobic and anaerobic metabolism in the cells subjected to OGD without treatment. The aerobic metabolism markedly improved in the adenosine pretreated cells, reaching 90% of the OCR values of the controls, and the anaerobic metabolism of the cells was indistinguishable from the controls. The mitochondrial potential also increased in the adenosine treated cells, but it was still lower than in the controls. We can postulate that the protons produced during anaerobic glucose breakdown but not used in the oxidative phosphorylation can account for the increase in the mitochondrial potential during the recovery phase.

Discussion

Oxygen-glucose deprivation induces cell death via various mechanisms in LLC-PK1 renal proximal tubule cells

In acute renal injury severe depletion of ATP occurs in the tubular cells as a result of hypoperfusion and it is assumed to play a central role in the pathogenesis of the disease [20]. The depletion of ATP in the tubular cells may induce cell death via apoptosis, necrosis and autophagy simultaneously [20, 21]. The degree of ATP depletion may determine whether the cells survive or die and also predict the overall outcome, since the higher ATP content promotes apoptosis (that requires more energy), and the lower ATP content of the cells induces necrosis [22, 23]. Historically, all these cell death processes were called necrosis in the kidney tubules and led to the nomenclature of acute tubular necrosis irrespective of the underlying molecular mechanism.

In the current project we prepared a cell culture model of acute renal injury that shares several common features with the human disease. Proximal tubular cells, the primary targets of ATN, were deprived of both oxygen and glucose for an extended period to mimic the ischemic origin of ATN (Fig. 1A). The tubular cells possess energy reserve that can be utilized in case of hypoperfusion, the cells can switch to solely anaerobic metabolism and produce sufficient ATP to survive and maintain the major cellular functions without any oxygen supply for a relatively long period (Fig. 1B). The severe decrease of renal blood flow not only stops the oxygen and glucose supply, but simultaneously reduces the filtrate production and functional needs of the tubular cells, reducing the ATP consuming transfer processes and thus promote the preservation of the cellular energy reserve over a long time period. Interestingly, in acute renal failure (ARF) patients urinary levels of brush border enzymes alkaline phosphatase (AP) and γ-glutamyl-transpeptidase (γ-GT) are increased already in the earliest samples, while urinary LDH concentration increases relatively late, 12-24 hours following the increase of γ-GT and AP [24]. Consistent with the clinical findings, OGD induced a cellular dysfunction in tubular cells, but increased LDH release and definitive cell death occurred only during the recovery period following the OGD (Fig. 2). The apoptotic nature of the cell death during the recovery period was supported by the

protective effect of caspase inhibitors and the inefficiency of inhibitors of PARP and necroptosis. Caspase activation is well documented in renal ischemia, and caspase inhibition also possesses a protective effect *in vivo* [25]. Active caspases stop various high energy requiring enzymatic processes by proteolytic cleavage of key enzymes, thus favor the energy preservation for the apoptotic process within the cells. This includes the cleavage of the DNA repair enzyme PARP that is widely associated with necrotic cell death. In our model the appearance of the 89 kDa PARP fragment, that is associated with caspase mediated cleavage [26], strongly followed the pattern of caspase activation detected by Western blotting using an active caspase-3 specific antibody and a fluorescent substrate-based activity assay (Fig. 3D). Mitochondrial dysfunction, depolarization and leakage (damage) are observed in ATN [27] and can be the initiator of caspase activation. Caspase activation and apoptosis are implicated in the cell death process in this model, albeit inhibition of caspase activity possesses a relatively minor benefit in our model system.

Tubular swelling is a typical finding in acute renal failure[28]. The swelling process also involves intracellular organelles and may be a contributor to the mitochondrial leakage and caspase activation.

Autophagy is a pathway for the degradation of proteins and cytoplasmic organelles that involves the rearrangement of subcellular membranes to deliver these substances to the lysosome where the sequestered material is degraded and recycled [29]. Autophagy is also implicated in the renal ischemia-reperfusion injury and is assumed to play a renoprotective role in the injury [30]. The protein and RNA content of the cell also represents an energy resource, as their controlled enzymatic degradation not only allows the re-utilization of the amino acids and nucleosides for novel protein synthesis, they can be further metabolized to produce ATP in the absence of glucose and fatty acids. The presence of autophagy in this models is supported by the appearance of proteolytic PARP fragments and by the fact that inhibition of nucleoside metabolism by EHNA or ABT 702 reduced the cellular ATP content and viability even in the absece of exogenous adenosine or inosine. A further benefit of autophagy is the removal of potentially harmful cell components. These include the DNA repair enzyme PARP and damage associated molecular pattern molecules (DAMPs) that induce inflammation if released from the cells [31]..The proteasome activation was found to play a protective role as the proteasome inhibitor bortezomib was shown to aggravate renal ischemia–reperfusion injury [32]. On the other hand, many of the proteases were also recognized as key contributors to cellular damage in ischemic renal injury, as the inhibition of these proteases or proteasomes confer protection against the renal damage. The proteases that are implicated include calpain [14], cathepsin [15] and granzyme B [16, 33], since inhibition of these proteases ameliorate renal ischemia-reperfusion injury. Interestingly, these proteases all cleave PARP. The presence of the specific PARP cleavage fragments strongly suggests activation of calpain, cathepsin and granzyme B during the reoxygenation period in our model (Fig. 3D). Since the activation of these proteases degrade PARP and prevent the PARP mediated energy depletion, these activities should represent a favorable profile in ischemia-reperfusion injury. The wide substrate specificity of these proteases certainly involves the degradation of other proteins, therefore they may counteract the recovery processes and enhance the injury.

PARP inhibition, which is also associated with the inhibition of necrosis in various diseases [34], was also found to be beneficial in renal ischemia-reperfusion but lacked any cytoprotective function in our model. PARP inhibition also exerts cytoprotection against oxidant induced renal injury *in vitro* in LLC-PK1 cells, but is ineffective in other models in which apoptosis is involved [35]. The cytoprotection by PARP inhibition is primarily associated with the prevention of the rapid depletion of the cellular NAD^+ and ATP pools by PARP overactivation in response to reactive oxygen species (ROS) mediated DNA damage. PARP-1 activation may also inhibit glycolysis via GAPDH PARylation that further aggravates the metabolic disorder in the post-hypoxic cells [36]. The loss of the mitochondrial membrane potential, the suppression of mitochondrial oxygen consumption lead to low cellular NAD^+ and ATP levels and low level of mitochondrial oxidant production immediately after the OGD in our model. These processes might be accounted for the inefficacy of the PARP inhibitor PJ34 in our model in the early phase of the injury, while the lack of functional PARP is the major cause during the later phase.

In our model, the complete absence of PARP-1 might be attributed to the lack of novel PARP protein synthesis as a result of the unfold protein response apart from the protease-mediated degradation. ATP depletion also increases the intracellular calcium level, activates the unfolded protein response, induces the dissociation of the Na^+-K^+ ATPase from the cytoskeleton [37, 38]. The increase in the intracellular calcium level may be attributable to the inability to sequester the calcium in the sarco-endoplasmic reticulum, as this process mediated by the sarco-endoplasmic reticulum calcium ATPase (SERCA) also requires ATP. The increased intracellular calcium level may increase the protease activity and can trigger endoplasmic reticulum (ER) stress. Renal energy depletion activates the unfolded protein response and ER stress [38], thus induces an inflammatory response and delays the recovery after the ischemia. In our model, we detected the loss of novel PARP-1 protein synthesis that can be a sign of ER stress, but the increase in GRP78 expression, a specific marker of the ER stress, was not detectable probably as a result of the poor reactivity of the available antibodies with the porcine GRP78 [39]. The actin microfilament and the microtubular system of the cells require considerable amount of energy even in resting cells, the energy consumption of this system may reach up to 30% of the total cellular ATP usage [40, 41]. The disturbed cytoskeletal system may be accounted for the loss of cellular polarity and the incorrect localization of various proteins. ATP depletion also involves the depletion of the GTP pool of the cells in renal ischemia-reperfusion injury [42] as GTP and ATP are mostly interconvertible within the cells, GTP repletion has a protective effect in renal ischemia-reperfusion injury [42]. Also ATP supplementation can restore the functional microfilament system in ATP depletion [43].

Necroptosis is a novel distinct form of cell death with characteristics similar to apoptosis and necrosis. It is implicated in cardiomyocyte and neural cell injury, and the blockade of necroptosis is protective against hypoxic or ischemia-reperfusion injury via delaying the opening of the mitochondrial permeability transition pore (MPTP) [44] [45]. Necroptosis has not yet been described in the kidney, and was not involved in the cell death in our model.

This model shows similarities to the human disease, but our screening approach also imposed certain limitations. We chose a well-characterized cell line to have uniform cellular responses throughout the screens. Immortalized cells may not show the same expression profile as the primary tubular cells. Also, tubular cells may show distinct responses in their physiological context in the kidney, that cannot be reproduced *in vitro* using one cell type. Our model completely lacked the oxidant producing infiltrating cells that contribute to the reperfusion injury. We also avoided extracellular acidosis in our model. During ischemia a gradual acidification and a rapid increase in the pCO_2 occur in the kidney simultaneously with the development of hypoxia and the decrease of nutrients [3, 46]. The major cause of hypercapnia is believed to be the continuing tricarboxylic acid cycle. CO_2 can penetrate the cellular membranes and rapidly induce a drop in both intra- and extracellular pH, using up the buffering capacity of the renal bicarbonate. During ARF, energy depletion and the loss of apical membrane transporters are responsible for the sustained acidosis and the bicarbonate reabsorption deficiency. The role of the acidification in renal failure is still controversial: early studies confirmed the protective function of acidosis [47], while the beneficial role of bicarbonate treatment is generally accepted to prevent metabolic acidosis. However, there is limited evidence of benefit of using bicarbonate based fluids over saline in the prevention of ARF [48]. We also tested the effect of acidic environment via the use of 18% CO_2 in the gas mixture that was used to induce hypoxia [46] and found only little difference in cell survival in our model (unpublished observation). As early correction of metabolic acidosis by bicarbonate supplementation is the currently accepted therapeutic approach, we performed our experiments using 5% CO_2 containing gas mixtures and culture medium containing 4.4 mM sodium bicarbonate to maintain stable pH and bicarbonate supply throughout the experiments.

Cell-based screening identifies adenosine as the most potent cytoprotective agent in OGD injury in LLC-PK1 cells

The Sigma LOPAC, a library of compounds comprising of various pharmacological activators and inhibitors, was chosen to screen for cytoprotective action in our cellular model of ATN. In the screens the viability was evaluated following the 24 hours of reoxygenation and glucose supplementation period to allow better discrimination of reversible dysfuntion and definitive cell death, and also to exclude those effects that only attain a transient functional gain (Fig. 4A). We employed two distinct strategies in our approach: (1) we simulated the usual clinical settings of the ischemic ATN by performing the OGD first and then normalizing the oxygen level and the glucose concentration simultaneously with the compound application following the OGD to mimic the situation when the therapeutics reach the renal parenchyma only if the renal blood flow is (partially) restored and (2) also prepared a model of ATN prevention by pre-treating the cells with the compounds immediately before the onset of the OGD that shows resemblance to the preventive approach when increased risk of renal injury occurs as a result of hypoperfusion (or a nephrotoxic agent) but the drug delivery to the renal tissue is still possible by systemic application via the renal circulation. Interestingly, those compounds that exerted cytoprotection in one setting were without effect in the other screen. The only notable exception was the purine nucleoside adenosine that showed the highest potency in the pre-treatment screen and was among the most protective compounds in the post-treatment assay

(Table 1). Disulfiram and allopurinol, compounds that may increase the endogenous adenosine concentration by interfering with its breakdown, also had mild protective effect.

In our model, both adenosine and inosine pretreatment increased the viability of the cells and decreased the LDH release in a dose dependent manner with similar potency. In this respect the cytoprotective potential of adenosine (and inosine) was mostly comparable to equal amount of glucose and also superior in the 30-100 μM concentration range. The cytoprotective effect of these purine nucleosides was also associated with a significant reduction in the OGD induced caspase activation (Fig. 5D), and adenosine also partially preserved the full-length PARP (Fig. 5E and F). This scenario strongly suggested that the adenosine-induced blockade of caspase activation prevented the apoptotic cell death and also reduced caspase mediated PARP cleavage. However, both caspase inhibition and the protection of PARP were incomplete, still adenosine exerted a near complete restoration of the viability. Also, the caspase inhibitor Z-VAD-fmk increased the viability by only approximately 10% in this model, suggesting that adenosine's protective action is not mediated merely via the inhibition of caspases. Interestingly, highly similar protective actions of adenosine were described in liver autophagy [49] and in glial cell injury [50], and the similar protective function of inosine in experimental renal injury was also described but the mechanism of action remained undiscovered [51].

Adenosine, inosine and hypoxanthine are postulated to reach high levels locally from endogenous sources in hypoxic tissues. Depending on the species and the length of the ischemia 3-10 fold increase occurs in the interstitial levels of both adenosine and inosine, reaching the low micromolar range [52-54], but their level rapidly decreases after the ischemia as their urinary excretion peaks early during the post-ischemic reperfusion period [53, 54]. Based on the protective action of adenosine in our hypoxia-reoxygenation injury and the published data claiming that these nucleosides are present at similar levels in the kidney during ischemia we presumed that drugs that enhance the protective effect of these purines may possess similar therapeutic potential in ARF. Therefore we re-screened the same compound library to search for compounds that potentiate adenosine's action if added simultaneously (prior to the OGD) or applied later during the reoxygenation. The protective compounds included PARP and NOS inhibitors. As adenosine also provides the cells with large amount of xanthine load it may promote ROS production by the xanthine oxidoreductase during the reoxygenation phase. Xanthine oxidoreductase (also known as xanthine: acceptor oxidoreductase) represents an interconvertible enzyme that is mainly present in the cells as xanthine: NAD^+ oxidoreductase (xanthine dehydrogenase or D form of the enzyme) and transfers electrons to NAD^+, however it is also converted to the more stable xanthine: oxygen oxidoreductase (xanthine oxidase or O type of the enzyme) during hypoxia [55, 56]. The depletion of NAD^+ and the accumulation of hypoxanthine may also block the xanthine dehydrogenase to some extent, but the lack of oxygen certainly inhibits xanthine oxidase during hypoxia. This enzyme transformed to xanthine oxidase by extended hypoxia uses oxygen as electron acceptor leading to superoxide generation. The superoxide may react with NO and form peroxynitrite, a highly toxic short-lived molecule. The oxidative and nitrosative damage caused by superoxide and peroxynitrite, in particular DNA strand breaks activate PARP during the reoxygenation or reperfusion [57]. Adenosine reduces the OGD-induced caspase activation and preserves functional PARP protein, thus it

is not surprising that PARP inhibition confers an additional benefit after adenosine supplementation. Also, compounds that reduce NO synthesis either by directly inhibiting NOS or by preventing the nuclear factor-κB mediated NOS expression showed protective effect.

L-aspartic acid represents the only compound that got into the “top ten” in both post-hypoxia screens, that clearly tells that the protective action of aspartate works in a parallel fashion to the adenosine-mediated viability increase. Aspartate is used for the proton transfer to feed the respiratory chain in the mitochondria and supports the energy production within the mitochondria. The summative nature of this function shows no overlap with adenosine's action and suggests that adenosine acts via different pathways, mostly independent from the mitochondrial respiration. Interestingly, L-aspartate is the amino acid that is utilized (next to bicarbonate and ammonia) during the *de novo* pyrimidine nucleotide synthesis, thus may function via multiple actions during the reoxygenation.

Adenosine exerts cytoprotection via ATP replenishment in renal proximal tubule cells

The protective effect of adenosine and inosine is well documented in *in vivo* models of ATN. This effect is mediated by the cell surface A_1 and A_2 adenosine receptors, as it was proved by various knockout models and studies using pharmacological inhibitors [58]. The action of adenosine on the renal vasculature and on the inflammatory cells is implicated in the renoprotective effect in ischemia-reperfusion. These receptors are also expressed by LLC-PK1 cells and show similar distribution as on proximal tubular cells *in vivo*: the majority of the A_1 receptors are localized to the basolateral membrane, whereas the A_2 receptors are present in greater quantity on the apical membrane [59]. Since none of the adenosine receptor antagonists blocked the protective action of inosine and adenosine (fig. 6), the protection exerted by them was independent of their action on the adenosine cell surface receptors in the current model suggesting an intracellular mechanism or the indirect action via the P2 type purinergic receptors. The P2 purinergic receptors have been implicated in the protective role of exogenous ATP in renal ischemia [60], but none of the direct P2 purinergic agonists (UDP, methylthio-ATP, 2-chloro-ATP) possessed a cytoprotective potential in our screens, it is unlikely that this mechanism plays a role in the adenosine and inosine mediated cytoprotection in our model.

Adenosine can be metabolized to inosine by adenosine deaminase (ADA). ADA and its binding or complexing protein, a membrane bound protein that specifically binds the enzyme, are present in the proximal tubules in the brush border of the cells [61]. The binding protein and ADA, as other brush border proteins, may detach from the proximal tubules and are excreted in the urine in ATN, thus can be used as early urinary markers [33, 62]. The similar efficacy of inosine and adenosine suggested that inosine is the active metabolite that exerts cytoprotection in this model and adenosine is merely a pre-drug that is converted to inosine by ADA. Inosine can be further metabolized to ribose-phosphate and thus utilized via the pentose phosphate pathway to generate ATP in an anaerobic fashion.

The incomplete blockade of the adenosine-mediated cytoprotection by ADA inhibition suggested the existence of other pathways participating in the cytoprotective action of adenosine and inosine. As adenosine can also be converted to adenosine monophosphate

(AMP) by adenosine kinase (AK) that uses ATP to phosphorylate adenosine and also generates ADP, we tested whether AK inhibition destroys the protective effect of adenosine. AK is highly expressed in the kidney and it is present in the proximal tubule cells in the brush border vesicles [63]. AK inhibition reduced the protective effect of adenosine with a similar potency to that of ADA inhibition and had comparable effect on the inosine mediated cytoprotection, but had only negligible effect on the glucose mediated protection.. However, adenosine and inosine still retained some of their protective action in the presence of the AK inhibitor ABT702. AK possesses another enzymatic function: it can mediate phosphotransfer between various nucleosides, thus can rapidly exchange GMP, IMP and dAMP to AMP in the presence of adenosine [63], explaining the similar effect of AK inhibition on adenosine and inosine in our model. This mechanism can be used to interconvert the various nucleosides according to the actual requirements, however, with the limitation of their availability and their near equal ratio within the cell. Similar to adenosine, guanosine was shown to exert protection in renal ischemia [42] and to increase GTP and to a lesser extent ATP levels, which also suggest the interconversion of these nucleosides during renal ischemic injury. We also tested the effect of nucleobases and various nucleosides, and found that none of the nucleobases (that lack the ribose-phosphate moiety) possessed a cytoprotective effect and the viability was only increased significantly by purine nucleosides (Fig. S1). The inefficacy of pyrimidine nucleosides may be explained by higher affinity of the transporters present on the cells for purine nucleosides.

The combined blockade of AK and ADA completely abolished the protective effect of both adenosine and inosine, which clearly underlines the coordinated actions of these enzymes in the protective function of inosine and adenosine. While the metabolism of these nucleosides via the pentose phosphate pathway can generate ATP, this process also requires ADP as phosphate acceptor. The reduction in the cellular ADP content may decrease the ATP generation, especially if the majority of ADP is further metabolized to adenosine and overall to ribose-phosphate. Thus adenosine (or inosine) supplementation can be simultaneously utilized for dual purposes: they provide the cells with the energy source in the form of their sugar part and they also block the breakdown of ADP (or may be used directly to produce AMP and ADP). The combined inhibition of AK and ADA even reduced the glucose mediated viability increase, which may reflect the importance of the endogenous adenosine and inosine production induced by hypoxia. The anaerobic glucose metabolism also requires ADP that may be the limiting factor of ATP production, thus the endogenous adenosine can supply AMP and ADP to convert the energy in the sugar to ATP, a readily available format for most purposes. Interestingly, AK inhibition by ABT702 also had a mild cytoprotective effect in the absence of glucose and exogenous adenosine and inosine in our screens (Table S1). In this case the very low level of sugars represents the limiting factor of energy production thus the endogenous nucleosides might be of use merely as sugars in the pentose phosphate pathway that is facilitated by the blockade of the AK pathway.

In our model, adenosine and inosine increased the viability comparable to equimolar amount of glucose, and the adenosine induced viability increase even surpassed the effect of glucose in the 30-100 μM range (Fig. 5), thus it is conceivable that the utilization of adenosine (and inosine) may be favorable even to the glycolytic glucose utilization under severe long-term ischemia or hypoxia or the cellular uptake mechanism of purine nucleosides is more

efficient than that of glucose. Furthermore, the cellular ATP content was higher after the hypoxia in the adenosine and inosine pretreated cells than in the cells that received equimolar amount of glucose pretreatment (Fig. 8A) supporting the higher ATP generating potential of these nucleosides.

Cells take up adenosine and inosine via nucleoside transporters, which are classified as equilibrative nucleoside transporters (ENT) that represent sodium-independent diffusion limited channels and concentrative nucleoside transporters (CNT) that are sodium dependent symporters [64, 65]. These transporters play a central role in the tubular reabsorption (and salvage) of nucleosides and their vectorial transfer in the proximal tubules [66] that function is also supported by their localization: the CNTs are present in the brush border on the apical membrane of the cell, while the ENTs are mainly present on the basolateral membrane. ENT1 and CNT3 are the two major isoforms on proximal tubular epithelium [67]. Adenosine is transported via ENT1 and CNT3 with apparent Km values of 40 μM and 15 μM, respectively [65]. Since dipyridamol had no negative effect on the adenosine-mediated cytoprotection in our model, but inhibits the ENT mediated transport, the purine nucleoside uptake rather occurs via the CNT3 transporter [68]. Still the CNT3 mediated adenosine transport is saturated by 100 μM adenosine, while in our model adenosine and inosine exerted cytoprotection in a concentration dependent manner with increased cell survival up to 1 mM (Fig. 5), thus it seems unlikely that the CNT3 mediated uptake is the sole mechanism responsible for the nucleoside uptake in these cells. A sodium-independent nucleobase transport system has been described in the PK15NTD and LLC-PK1 porcine kidney tubular cells that also transports purine nucleosides, but with approximately 1,000-fold lower affinity than nucleobases, showing an apparent Km value of 5 mM for adenosine [69-71]. This transport is resistant to dipyridamole but sensitive to papaverine [70]. Since 30 μM papaverine completely abolished the cytoprotective effect of adenosine in our screens (Table S1), we suppose that the cellular uptake of adenosine and inosine may also occur via the papaverine-sensitive nucleobase transporters in the renal proximal tubule cells.

Glucose uptake is mediated by either the sodium-coupled glucose transporter (SGLT) or the sodium-independent facilitated glucose transporter (GLUT) in the LLC-PK1 cells [72]. The GLUT transporter is localized mainly to the basolateral membrane, while the SGLT is present on the apical membrane that reflects their physiological function: SGLT is involved in the glucose reabsorption from the tubule lumen and GLUT is implicated in the glucose uptake from the circulation [73]. Only one isoform of each (SGLT1 and GLUT1) was identified in this cell line and their expression is shown to be regulated by the glucose concentration: exposure to high glucose downregulates both transporters, complete deprivation or low levels of glucose upregulates GLUT1 while SGLT expression is highest between 5-10 mM glucose and it almost completely disappears after glucose deprivation [72]. The sodium-independent transport is also shown to be upregulated after glucose deprivation [73], showing that the GLUT mediated transport is dominant in glucose deprivation.

Both glucose and the purine nucleoside uptake are partly connected to sodium transport that necessitates the active removal of sodium from the cell via the basolateral Na^+-K^+ ATPase. The sodium-potassium exchanger works with a 3:2 (or as low as 3:0) sodium:potassium

stocichiometry per ATP hydrolyzed [74]. Ischemic injury and energy depletion disrupt the polarized phenotype of the tubular cells and also disintegrate the barrier formed by the tubular epithelium [75]. During this process the distribution of many transporters and receptors undergo rapid changes including the basolateral Na^+-K^+ ATPase [75] that is needed for all sodium-coupled transport.

In contrast to glucose phosphorylation by hexokinase that requires ATP, the conversion of inosine to ribose-phosphate (and hypoxanthine) does not need ATP, but it needs inorganic phosphate. Thus, the glucose utilization via glycolysis yields 2 ATP molecules and 2 NADH and H^+ per glucose, if sodium transport is not calculated, while adenosine or inosine may yield 3 ATP molecules (10/3 ATP produced per ribose-phosphate minus 1/3 ATP required for transport at 1:1 sodium:nucleoside transfer ratio). Since the resulting NADH and H^+ cannot be converted to ATP without oxygen, NADH generation can be detrimental during hypoxia if it completely exhausts the cellular NAD^+ pool. Furthermore, glucose deprivation downregulates the luminal glucose transporters that may aggravate the intracellular glucose deficiency, while the purine nucleoside transporters are highly efficient at low nucleoside concentrations.

The cellular ATP content is severely diminished after the OGD in the proximal tubule epithelial cells in our model, reaching values below 10% of the control ATP concentration. Adenosine or inosine pretreatment also increased the rate of the cellular ATP pool regeneration that was completely restored by 24 hours, while the presence of equimolar amount of glucose during the hypoxia supported the recovery of no more than 60% of ATP content by that time. Adenosine also had a protective effect in our screens when applied following the OGD. Both ADA and AK appeared to participate in the cellular energy production, since the post-hypoxic ADA and AK inhibition both reduced the ATP concentration in the adenosine and inosine pretreated and also in the glucose pretreated cells, but AK inhibition had a more pronounced effect. Thus, it is conceivable that AK is implicated in the interconversion of nucleosides and the regeneration of the AMP and ADP content of the cells, while ADA is still needed in the presence of glucose to promote the usage of nucleosides and their ribose part through the pentose-phosphate pathway. The nucleosides and ribose probably also comes from the degradation of RNA as part of the autophagy after the hypoxia. The need for the pentose phosphate pathway may be justified by the lower ATP producing capacity of the mitochondria after hypoxia, the inhibition of glycolysis as seen in the reperfusion injury *in vivo* [36] and the lower NAD^+ requirement of anaerobic nucleoside utilization. We detected a severe blockade of the mitochondrial respiration after the OGD, and a near complete loss of the mitochondrial potential (total capacity) (Fig. 9). Even the adenosine-treated cells that showed comparable level of anaerobic metabolism (proton production) to the control cells after the hypoxia, showed a significantly reduced mitochondrial basal respiration and an even greater decrease in the mitochondrial reserve capacity. Both the aerobic and anaerobic metabolism were severely damaged in cells undergoing OGD without adenosine pretreatment and showed very little measurable improvement in the recovery period in spite of the presence of glucose and oxygen in agreement with the impaired ATP regeneration in these cells. While the mitochondrial respiration steadily increased in the adenosine pretreated cells during the

recovery period, the basal mitochondrial respiration still remained under the level of the control cells. These data also support the significance of the anaerobic metabolism in the posthypoxic cells. Thus, lactate, as it requires mitochondrial metabolism to produce ATP, is an inferior energy source for the kidney after ischemia, yet it is widely used in intensive care. It should be noted, however, that the tissue content of nucleosides rapidly decreases after hypoxia in the kidney as these molecules are also excreted in the urine [52, 54], if they are not taken up by the cells from the glomerular filtrate. The loss of the tubular barrier, cell shedding and the loss of the cellular polarity may destine them to perform the transport processes excessively, as the vectoral transport of many compounds are inefficient since they can re-enter the tubule lumen from the interstitial space via the intercellular leakage. Additionally, the dislocation of the transporters may induce reverse transport processes that counteract the physiological transfer direction and reduce the overall efficiency. These processes may further enhance the cellular ATP depletion after the hypoxia and contribute to cellular injury. The detachment of the brush border with many of transporters in the apical membrane was also described in ATN [76] and it certainly reduces the ATP usage via the decrease in the transport processes, but may also lead to the loss of the brush border enzymes ADA and AK. Therefore the reperfusion not only reduces the levels of the nucleosides that possess a beneficial role in the post-hypoxic regeneration, during this period the proximal tubules may lose their transport system required for the uptake of the extracellular nucleosides and the enzymes necessary for conversion of the nucleosides to ATP which all advise for an early purine nucleoside therapy in ATN.

Conclusion

In a cellular model of ATN we screened a library of compounds possessing known biological function searching for a novel function of these drugs, a renoprotective action in hypoxia. The purine nucleoside adenosine not only showed the highest cytoprotective potential in the pre-hypoxia setting, but it represented the only compound in the tested compound library that exerted a marked cytoprotective action both if applied after the hypoxic challenge or before the onset of the hypoxia. Inosine, the metabolite of adenosine exerted similar protection and the viability increase these compounds achieved was comparable to the effect of equimolar glucose. The cell surface adenosine receptors that were implicated in the renoprotective action of adenosine in various *in vivo* models, did not play a part in adenosine-and inosine-mediated cytoprotection in this model. The protective action of these purine nucleosides was solely dependent on their intracellular metabolism by ADA and AK. Both the ADA-mediated conversion of adenosine to inosine and the AK-mediated phosphorylation of adenosine or the phosphotransfer function of the enzyme were essential for the full protective effect of adenosine. These pathways complemented each other in supporting the ATP production of the cells both during the hypoxia and the following recovery period that yet again provided access to glucose and oxygen. Surprisingly, in the proximal tubule cells these nucleosides were better sources of energy under the hypoxic condition than similar amount of glucose. Although, the ATP content of the cells also decreased in the adenosine treated cells, nucleoside supplementation accelerated the recovery of the cellular ATP pool and completely restored the cellular viability in an OGD induced injury that resulted in 80% decrease in viability in non–treated

cells. These results also underline the central role of the fluctuation of the cellular energy resources and the significance of the metabolic changes that occur in severe ischemia and give us an example how these processes may determine the cell fate in the subsequent reperfusion period. Also, the energetic basis of renal injury and the multiple downstream components involved in the tissue damage emphasize that novel pharmacological approaches are necessitated for successful therapy in ATN that do not necessarily involve a classic agonist/antagonist or one drug-one target approach, and instead of confirming the short-term benefits of interventions rather focus on the overall outcome of the disease, and aim the better preservation of the proximal tubule cells and functional recovery of tubules. The protective effect of direct ATP replenishment has previously been observed in various experimental settings [60, 77], although the penetration of ATP through the cell membrane is still questionable [78]. However, no cell permeable alternatives or other methods were systematically searched for that aim the rapid restoration of the ATP content of the proximal tubule cells. Thus, the ATP-restoring capacity of purine nucleosides may embody an essentially novel approach in which the control of the cellular metabolism represents the pharmacological target and a broadly functional substrate is the drug treatment. Also the similar efficacy of other purine nucleosides and the additional benefits conferred by aspartic acid suggests that a combination therapy with various purine nucleosides and amino acids is a feasible alternative of a single nucleoside therapy that may be further supplemented with the blockade of various inhibitors of the high energy consumptive non-essential cellular pathways.

Supplementary Material

Refer to Web version on PubMed Central for supplementary material.

Acknowledgements

This work was supported by a grant from the Oszkar Asboth project grant of the National Office for Research and Technology (Budapest, Hungary) and by a grant from the National Institutes of Health (R01GM060915) to C.S.

Abbreviations

Acetyl-CoA	acetyl coenzyme A
ADA	adenosine deaminase
ADP	adenosine diphosphate
AK	adenosine kinase
AMP	adenosine monophosphate
ADP	adenosine diphosphate
ATP	adenosine triphosphate
CTL	control
ECAR	extracellular acidification rate
ER	endoplasmatic reticulum

GTP	guanosine triphosphate
NAD^+	nicotinamide adenine dinucleotide
NO	nitric oxide
OCR	oxygen consumption rate
OGD	oxygen-glucose deprivation
PARP	poly(ADP-ribose) polymerase
PRE	pre-treatment
POST	post-treatment
SERCA	sarco-endoplasmatic reticulum calcium ATP-ase

References

1. Brown JR, Block CA, Malenka DJ, O'Connor GT, Schoolwerth AC, Thompson CA. JACC. Cardiovascular interventions. 2009; 2:1116–1124. [PubMed: 19926054]
2. Jones DR, Lee HT. Current opinion in anaesthesiology. 2007; 20:106–112. [PubMed: 17413392]
3. Russ AL, Haberstroh KM, Rundell AE. Experimental and molecular pathology. 2007; 83:143–159. [PubMed: 17490640]
4. Lieberthal W, Nigam SK. American journal of physiology. Renal physiology. 2000; 278:F1–F12. [PubMed: 10644651]
5. Fishbane S, Durham JH, Marzo K, Rudnick M. Journal of the American Society of Nephrology : JASN. 2004; 15:251–260. [PubMed: 14747371]
6. Diethelm AG, Wilson SJ. The Journal of surgical research. 1971; 11:265–276. [PubMed: 4934949]
7. Portilla D, Schnackenberg L, Beger RD. Seminars in nephrology. 2007; 27:609–620. [PubMed: 18061843]
8. An WF, Tolliday NJ. Methods in molecular biology. 2009; 486:1–12. [PubMed: 19347612]
9. Kepp O, Galluzzi L, Lipinski M, Yuan J, Kroemer G. Nature reviews. Drug discovery. 2011; 10:221–237. [PubMed: 21358741]
10. Gero D, Modis K, Nagy N, Szoleczky P, Toth ZD, Dorman G, Szabo C. International journal of molecular medicine. 2007; 20:749–761. [PubMed: 17912470]
11. Suzuki K, Olah G, Modis K, Coletta C, Kulp G, Gerö D, Szoleczky P, Chang T, Zhou Z, Wu L, Wang R, Papapetropoulos A, Szabo C. Proceedings of the National Academy of Sciences. 2011
12. Chaitanya GV, Babu PP. Cellular and molecular neurobiology. 2009; 29:563–573. [PubMed: 19225880]
13. Aikin R, Rosenberg L, Paraskevas S, Maysinger D. Journal of molecular medicine. 2004; 82:389–397. [PubMed: 15105993]
14. Chatterjee PK, Brown PA, Cuzzocrea S, Zacharowski K, Stewart KN, Mota-Filipe H, McDonald MC, Thiemermann C. Kidney international. 2001; 59:2073–2083. [PubMed: 11380809]
15. Shimoda N, Fukazawa N, Nonomura K, Fairchild RL. The American journal of pathology. 2007; 170:930–940. [PubMed: 17322378]
16. Trapani JA, Jans DA, Jans PJ, Smyth MJ, Browne KA, Sutton VR. The Journal of biological chemistry. 1998; 273:27934–27938. [PubMed: 9774406]
17. Szabo, C.; Gero, D.; Hasko, G. Adenosine receptors: therapeutic aspects for inflammatory and immune diseases. Hasko, G.; Cronstein, BN.; Szabo, C., editors. CRC Press; 2007. p. 237-256.
18. Chen SF, Stoeckler JD, Choi HS, Burgess FW, Marcaccio EJ Jr. Steen PA, Berman SF, Parks RE Jr. Panzica RP, Abushanab E. Biochemical pharmacology. 1982; 31:3955–3960. [PubMed: 7159473]

19. Modis K, Gero D, Nagy N, Szoleczky P, Toth ZD, Szabo C. British journal of pharmacology. 2009; 158:1565–1578. [PubMed: 19906119]
20. Sharfuddin AA, Molitoris BA. Nature reviews. Nephrology. 2011; 7:189–200. [PubMed: 21364518]
21. Lieberthal W, Menza SA, Levine JS. The American journal of physiology. 1998; 274:F315–327. [PubMed: 9486226]
22. Formigli L, Papucci L, Tani A, Schiavone N, Tempestini A, Orlandini GE, Capaccioli S, Orlandini SZ. Journal of cellular physiology. 2000; 182:41–49. [PubMed: 10567915]
23. Leist M, Single B, Castoldi AF, Kuhnle S, Nicotera P. The Journal of experimental medicine. 1997; 185:1481–1486. [PubMed: 9126928]
24. Westhuyzen J, Endre ZH, Reece G, Reith DM, Saltissi D, Morgan TJ. Nephrology, dialysis, transplantation : official publication of the European Dialysis and Transplant Association - European Renal Association. 2003; 18:543–551.
25. Chatterjee PK, Todorovic Z, Sivarajah A, Mota-Filipe H, Brown PA, Stewart KN, Cuzzocrea S, Thiemermann C. European journal of pharmacology. 2004; 503:173–183. [PubMed: 15496312]
26. Rheaume E, Cohen LY, Uhlmann F, Lazure C, Alam A, Hurwitz J, Sekaly RP, Denis F. The EMBO journal. 1997; 16:6346–6354. [PubMed: 9351817]
27. Halestrap AP. Biochemical Society transactions. 2006; 34:232–237. [PubMed: 16545083]
28. Majno G, Joris I. The American journal of pathology. 1995; 146:3–15. [PubMed: 7856735]
29. Levine B, Kroemer G. Cell. 2008; 132:27–42. [PubMed: 18191218]
30. Jiang M, Liu K, Luo J, Dong Z. The American journal of pathology. 2010; 176:1181–1192. [PubMed: 20075199]
31. Lotze MT, Zeh HJ, Rubartelli A, Sparvero LJ, Amoscato AA, Washburn NR, Devera ME, Liang X, Tor M, Billiar T. Immunological reviews. 2007; 220:60–81. [PubMed: 17979840]
32. Huber JM, Tagwerker A, Heininger D, Mayer G, Rosenkranz AR, Eller K. American journal of physiology. Renal physiology. 2009; 297:F451–460. [PubMed: 19458122]
33. Trof RJ, Di Maggio F, Leemreis J, Groeneveld AB. Shock. 2006; 26:245–253. [PubMed: 16912649]
34. Gero D, Szabo C. Current opinion in anaesthesiology. 2008; 21:111–121. [PubMed: 18443476]
35. Filipovic DM, Meng X, Reeves WB. The American journal of physiology. 1999; 277:F428–436. [PubMed: 10484526]
36. Devalaraja-Narashimha K, Padanilam BJ. Journal of the American Society of Nephrology : JASN. 2009; 20:95–103. [PubMed: 19056868]
37. Caplanusi A, Fuller AJ, Gonzalez-Villalobos RA, Hammond TG, Navar LG. American journal of physiology. Renal physiology. 2007; 293:F533–540. [PubMed: 17522266]
38. Fougeray S, Bouvier N, Beaune P, Legendre C, Anglicheau D, Thervet E, Pallet N. Cell death & disease. 2011; 2:e143. [PubMed: 21490675]
39. Liu H, Bowes RC 3rd, van de Water B, Sillence C, Nagelkerke JF, Stevens JL. The Journal of biological chemistry. 1997; 272:21751–21759. [PubMed: 9268304]
40. Desai A, Mitchison TJ. Annual review of cell and developmental biology. 1997; 13:83–117.
41. Bernstein BW, Bamburg JR. The Journal of neuroscience : the official journal of the Society for Neuroscience. 2003; 23:1–6. [PubMed: 12514193]
42. Kelly KJ, Plotkin Z, Dagher PC. The Journal of clinical investigation. 2001; 108:1291–1298. [PubMed: 11696573]
43. Kellerman PS. The Journal of clinical investigation. 1993; 92:1940–1949. [PubMed: 8408646]
44. Degterev A, Huang Z, Boyce M, Li Y, Jagtap P, Mizushima N, Cuny GD, Mitchison TJ, Moskowitz MA, Yuan J. Nature chemical biology. 2005; 1:112–119. [PubMed: 16408008]
45. Han W, Xie J, Li L, Liu Z, Hu X. Apoptosis : an international journal on programmed cell death. 2009; 14:674–686. [PubMed: 19288276]
46. Hotter G, Palacios L, Sola A. Laboratory investigation; a journal of technical methods and pathology. 2004; 84:213–220.

47. Bonventre JV, Cheung JY. The American journal of physiology. 1985; 249:C149–159. [PubMed: 4014448]
48. Kellum JA, Leblanc M, Venkataraman R. Clinical evidence 2008. 2008
49. Samari HR, Seglen PO. The Journal of biological chemistry. 1998; 273:23758–23763. [PubMed: 9726984]
50. Jurkowitz MS, Litsky ML, Browning MJ, Hohl CM. Journal of neurochemistry. 1998; 71:535–548. [PubMed: 9681443]
51. Fernando AR, Gunter PA, Hendry WF, Smith AF, Watkinson LE, Wickham JE. British journal of urology. 1979; 51:167–172. [PubMed: 465981]
52. Baranowski RL, Westenfelder C. The American journal of physiology. 1994; 267:F174–182. [PubMed: 8048558]
53. Miller WL, Thomas RA, Berne RM, Rubio R. Circulation research. 1978; 43:390–397. [PubMed: 679422]
54. Nishiyama A, Kimura S, He H, Miura K, Rahman M, Fujisawa Y, Fukui T, Abe Y. American journal of physiology. Renal physiology. 2001; 280:F231–238. [PubMed: 11208598]
55. Kaminski ZW, Pohorecki R, Ballast CL, Domino EF. Circulation research. 1986; 59:628–632. [PubMed: 3469036]
56. Linder N, Martelin E, Lapatto R, Raivio KO. American journal of physiology. Cell physiology. 2003; 285:C48–55. [PubMed: 12637268]
57. Gero D, Szabo C. Current pharmaceutical design. 2006; 12:2903–2910. [PubMed: 16918420]
58. Vallon V, Osswald H. Handbook of experimental pharmacology. 2009:443–470. [PubMed: 19639291]
59. LeVier DG, McCoy DE, Spielman WS. The American journal of physiology. 1992; 263:C729–735. [PubMed: 1329540]
60. Kribben A, Feldkamp T, Horbelt M, Lange B, Pietruck F, Herget-Rosenthal S, Heemann U, Philipp T. The Journal of laboratory and clinical medicine. 2003; 141:67–73. [PubMed: 12518170]
61. Schrader WP, West CA, Rudofsky UH, Samsonoff WA. The journal of histochemistry and cytochemistry : official journal of the Histochemistry Society. 1994; 42:775–782. [PubMed: 8189039]
62. Bagshaw SM, Langenberg C, Haase M, Wan L, May CN, Bellomo R. Intensive care medicine. 2007; 33:1285–1296. [PubMed: 17487471]
63. Sayos J, Solsona C, Mallol J, Lluis C, Franco R. The Biochemical journal 297. 1994; (Pt 3):491–496.
64. Rose JB, Coe IR. Physiology. 2008; 23:41–48. [PubMed: 18268364]
65. Molina-Arcas M, Casado FJ, Pastor-Anglada M. Current vascular pharmacology. 2009; 7:426–434. [PubMed: 19485885]
66. Lai Y, Bakken AH, Unadkat JD. The Journal of biological chemistry. 2002; 277:37711–37717. [PubMed: 12097333]
67. Damaraju VL, Elwi AN, Hunter C, Carpenter P, Santos C, Barron GM, Sun X, Baldwin SA, Young JD, Mackey JR, Sawyer MB, Cass CE. American journal of physiology. Renal physiology. 2007; 293:F200–211. [PubMed: 17409283]
68. Ritzel MW, Ng AM, Yao SY, Graham K, Loewen SK, Smith KM, Ritzel RG, Mowles DA, Carpenter P, Chen XZ, Karpinski E, Hyde RJ, Baldwin SA, Cass CE, Young JD. The Journal of biological chemistry. 2001; 276:2914–2927. [PubMed: 11032837]
69. Griffith DA, Jarvis SM. The Journal of biological chemistry. 1993; 268:20085–20090. [PubMed: 8376366]
70. Hoque KM, Chen L, Leung GP, Tse CM. American journal of physiology. Regulatory, integrative and comparative physiology. 2008; 294:R1988–1995.
71. Yamamoto S, Inoue K, Murata T, Kamigaso S, Yasujima T, Maeda JY, Yoshida Y, Ohta KY, Yuasa H. The Journal of biological chemistry. 2010; 285:6522–6531. [PubMed: 20042597]
72. Ohta T, Isselbacher KJ, Rhoads DB. Molecular and cellular biology. 1990; 10:6491–6499. [PubMed: 2247068]

73. Mullin JM, McGinn MT, Snock KV, Kofeldt LM. The American journal of physiology. 1989; 257:F11–17. [PubMed: 2750915]
74. Cox TC, Helman SI. The Journal of general physiology. 1986; 87:467–483. [PubMed: 2420919]
75. Molitoris BA. The American journal of physiology. 1991; 260:F769–778. [PubMed: 2058700]
76. Racusen LC, Fivush BA, Li YL, Slatnik I, Solez K. Laboratory investigation; a journal of technical methods and pathology. 1991; 64:546–556.
77. Gaudio KM, Taylor MR, Chaudry IH, Kashgarian M, Siegel NJ. Kidney international. 1982; 22:13–20. [PubMed: 7120752]
78. Chaudry IH. The Yale journal of biology and medicine. 1982; 55:1–10. [PubMed: 7051582]

Highlights

- We model renal ischemia-reperfusion injury in LLC-PK1 cells
- We study the viability changes to compounds of LOPAC library
- Adenosine exerts protection against oxygen-glucose deprivation injury
- Adenosine receptors do not participate in the protective effect of adenosine
- Adenosine kinase and adenosine deaminase play important roles in the cytoprotection

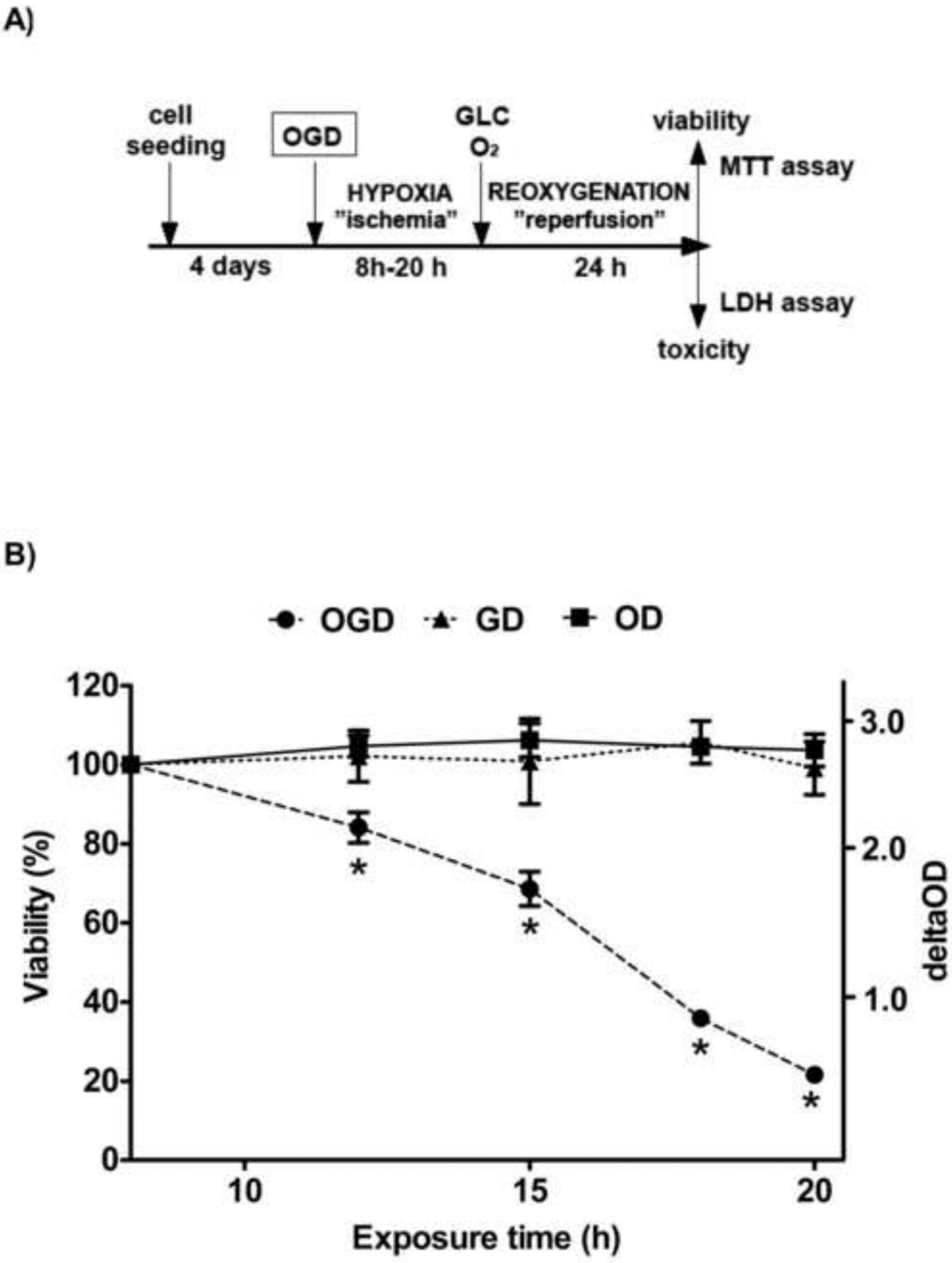

Figure 1. The experimental design of hypoxic tubular injury and the time-course of the viability decrease in LLC-PK1 cells

LLC-PK1 proximal tubule cells were grown to form confluent monolayer and then subjected to either glucose (GD) or oxygen (OD) or combined oxygen and glucose deprivation (OGD) for the designated time period to mimic ischemia. Reperfusion injury was imitated by resupplying glucose and oxygen (5.5 mM glucose, 20% oxygen) for 24 hours prior to evaluation of cellular viability and cell death by the MTT and LDH assays (A). Viability values are shown that were calculated relative to control cells maintained under

normoglycemia and normoxia for the same length (B). (Data are mean ± SD values, *$p<0.05$ compared to CTL).

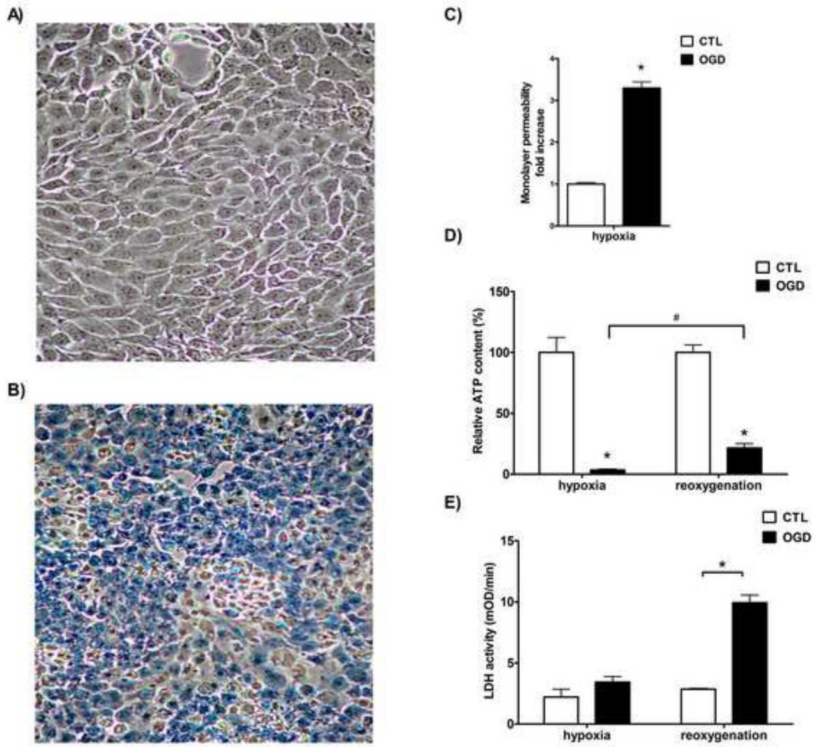

Figure 2. Cellular dysfunction, ATP depletion and cell death after OGD

LLC-PK1 cells were subjected to hypoxia with excess glucose (CTL, A) or with simultaneous glucose deprivation (OGD, B) for 20 hours and were stained with trypan blue. Representative micrographs are shown. The permeability of the monolayer was measured immediately after hypoxia and fold increase is shown relative to CTL (C). Cellular ATP content (D) was measured from cell lysates prepared immediately following the hypoxia ("hypoxia") and after a 1-day-long recovery ("reoxygenation"). Relative ATP contents are shown compared to controls. LDH activity was measured in cell culture supernatant in samples taken immediately after the hypoxia or after the 24 hour-long reoxygenation (E). The measured enzyme activity values are shown in mOD/min. (Data are shown as mean ± SD values, *$p<0.05$ compared to CTL, #$p<0.05$ compared to the respective post-hypoxia value).

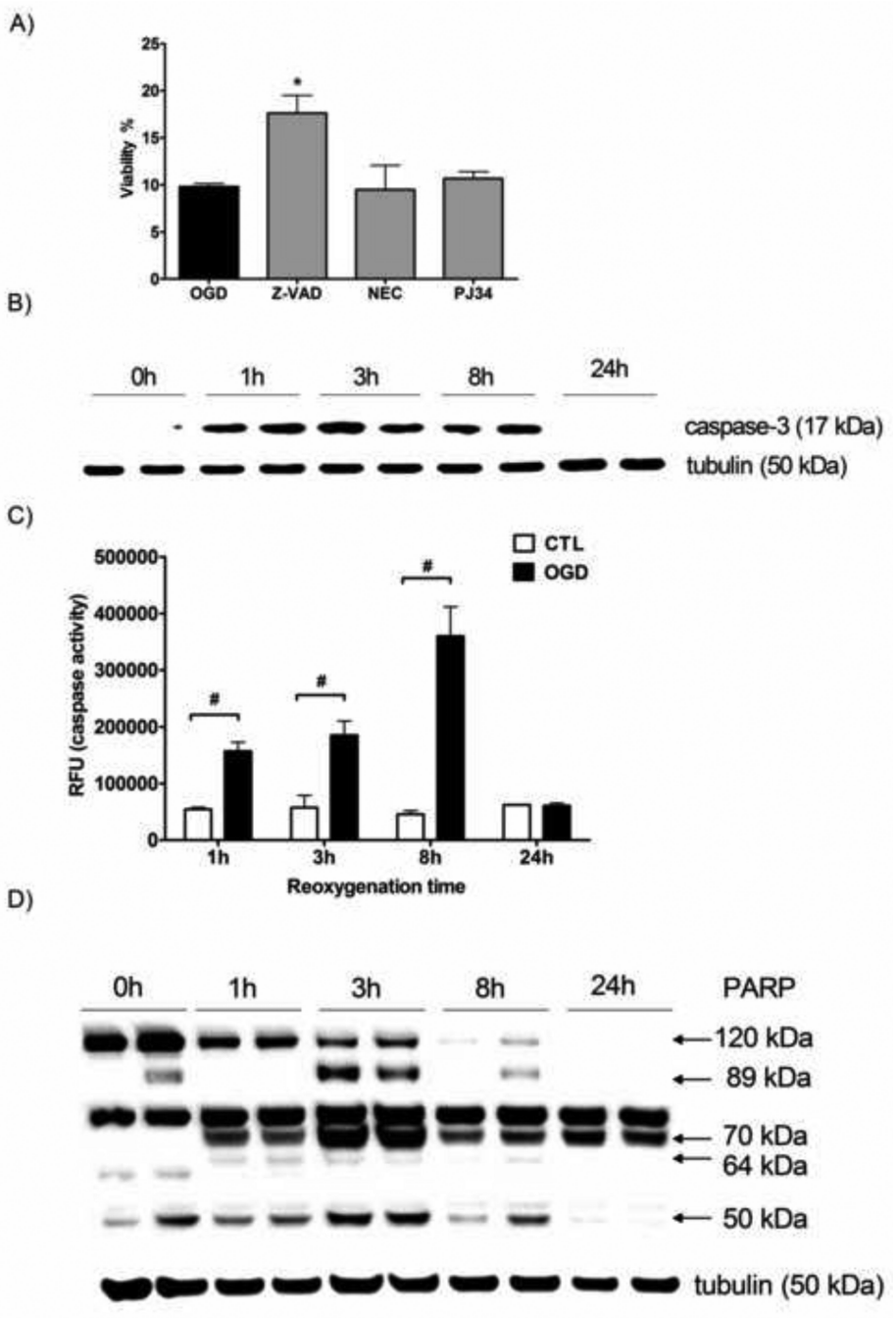

Figure 3. Caspase-3 activation and PARP cleavage following ATP depletion

LLC-PK1 cells were subjected to OGD for 20 hours, then resupplied with oxygen and glucose and treated with Z-VAD-fmk (Z-VAD), necrostatin-1 (NEC) or PJ 34 at 10 μM. The viability was measured after the 24 hour-long recovery period by the MTT assay (A). Cells were subjected to 20 hour-long OGD and maintained under normoxia with glucose supplementation for the indicated time for the detection of active caspase-3 protein (B), caspase activity (C) and PARP protein (D). Representative Western blot images with tubulin signal as loading control are shown (B and D). Caspase-3 activity was measured with

fluorescent substrate and relative fluorescence (RFU) values of the cleavage product are shown. (Mean ± SD values are shown, *p<0.05 compared to OGD, #p<0.05 compared to CTL).

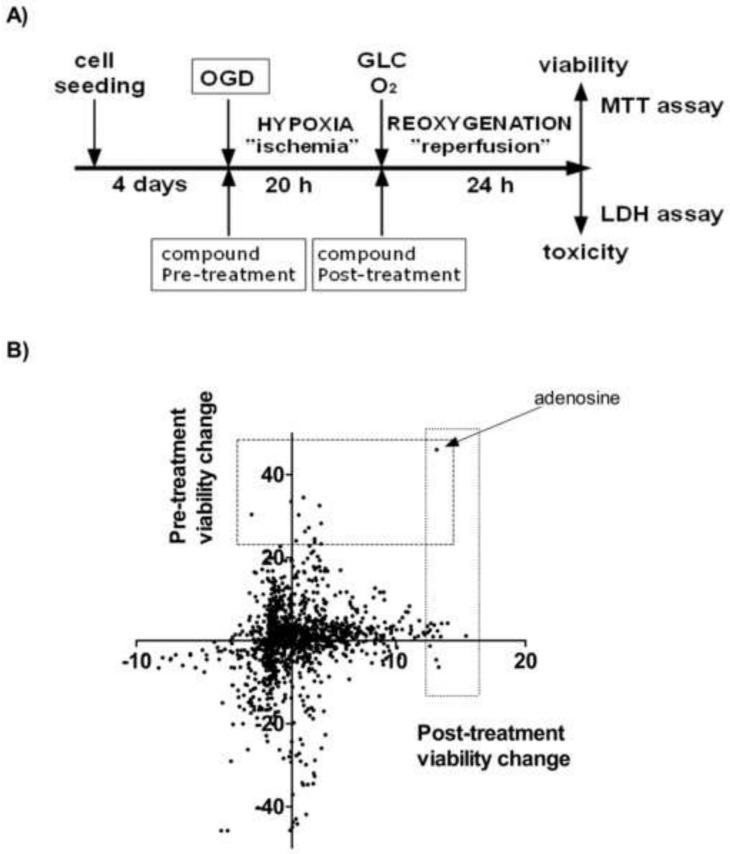

Figure 4. The experimental design of the screens and the compound-induced viability changes in the assays

LLC-PK1 proximal tubule cells were grown to form confluent monolayer and then subjected to OGD for 20 hours to mimic ischemia. Reperfusion injury was imitated by glucose and oxygen re-supplementation for 24 hours, then the cell survival was evaluated by the MTT and LDH assays. Test compounds were screened for cytoprotection by treating the cells either prior to the OGD ("Pre-treatment") or following the OGD ("Post-treatment) (A). The viability changes induced by the compound treatment are shown as percent values compared to the vehicle treated cells (zero value) on the dot plot. The effect of the post-treatment is shown on the x axis and the changes in the pre-treatment screen are represented on the y axis (B). The screens were performed in replicates and the average values are shown.

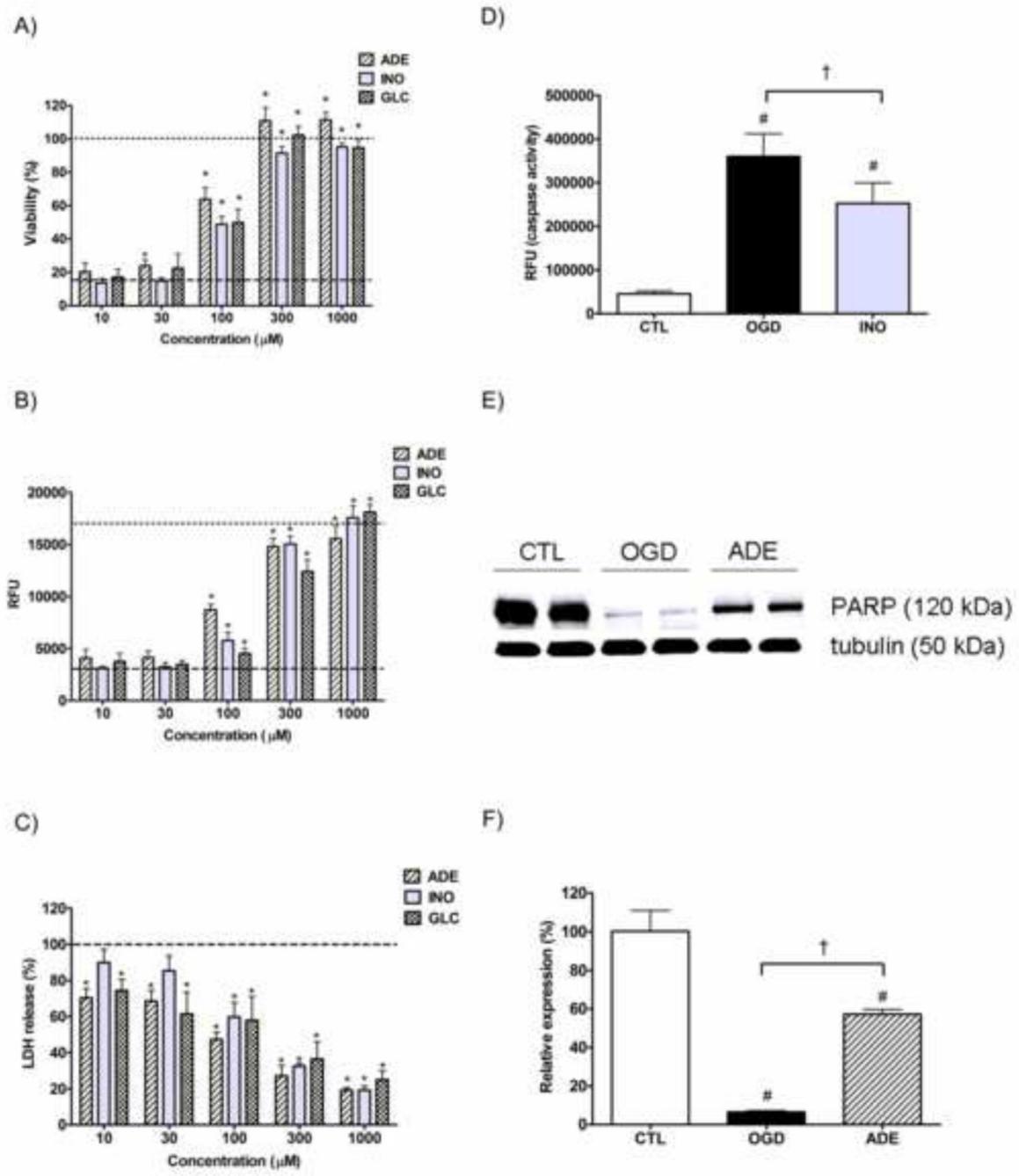

Figure 5. The protective actions of adenosine and inosine against the OGD induced proximal tubule injury

LLC-PK1 cells were subjected to 20 hour-long OGD in presence of the indicated concentration adenosine, inosine or glucose and then re-supplemented with glucose and oxygen for 24 hours. The viability was measured by the MTT (A) and alamar blue (B) assays, the LDH release was evaluated by measuring the LDH activity in the supernatant (C). The viability value of the OGD group is labeled with the dashed line, and the CTL viability is shown as dotted line. The decrease in LDH release is shown as percent value of the LDH activity of the vehicle treated cells (OGD). Cells were subjected to 20 hour-long

OGD with the absence (OGD) or presence of 100 μM inosine (INO) and caspase-3 activity was measured after 8 hours of reoxygenation. Caspase-3 activity was measured with fluorescent substrate and relative fluorescence (RFU) values of the cleavage product are shown (D). Cells were subjected to 20 hour-long OGD with the absence (OGD) or presence of 300 μM adenosine (ADE) and the amount of full-length PARP-1 was evaluated by Western blotting (E and F). Representative blot of PARP-1 and normalization signal tubulin (E) and results of the densitometric analysis (F) are shown. The bar graph represents the PARP-1 (120 kDa) signal normalized to tubulin as relative PARP-1 expression compared to the CTL. (Data are shown as mean ± SD values, *$p<0.05$ compared to OGD #$p<0.05$ compared to CTL, †$p<0.05$ compared to OGD group).

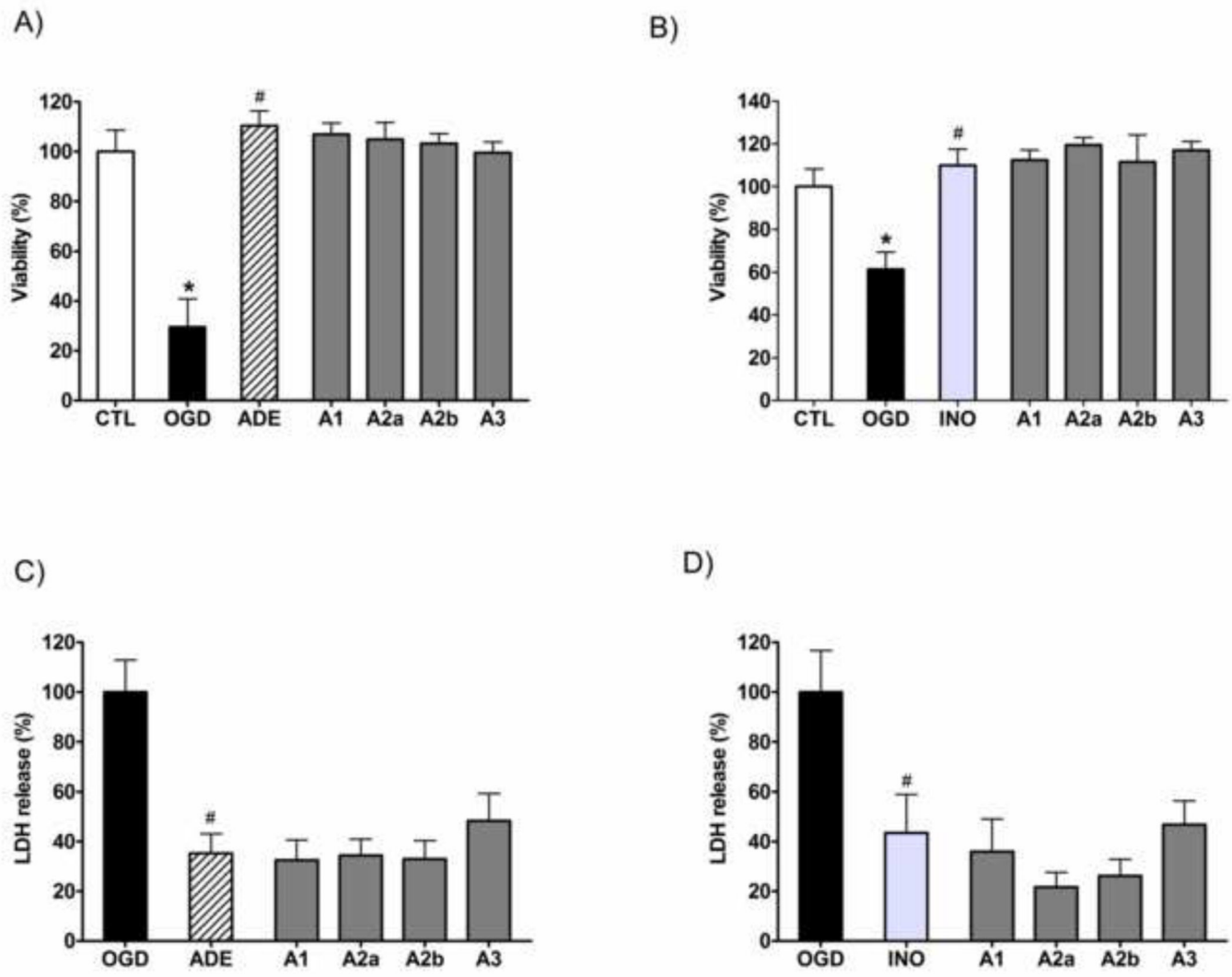

Figure 6. The effects of adenosine receptor antagonist on adenosine- and inosine-mediated protection in LLC-PK1 cells subjected to OGD

The cells were exposed to 20 hour-long OGD followed by a 24-hour-long recovery period in the presence of 1,000 μM of adenosine (ADE) (A,C) or inosine (INO) (B,D) and the respective receptor antagonists (3 μM): A_1 receptor antagonist CDPX (A_1), A_{2A} receptor antagonist 8-(3-Chlorostyryl)caffeine (A_{2A}), A_{2B} receptor antagonist alloxazine (A_{2B}), A_3 receptor antagonist MRS 1523 (A_3). The cellular viability was evaluated by the MTT assay (A, B) and expressed as percent values of controls. LDH activity (C,D) was measured in the supernatant and shown as percent value of the vehicle treated controls (OGD). Mean ± SD values are shown. (*$p<0.05$ compared to CTL, #$p<0.05$ compared to OGD.)

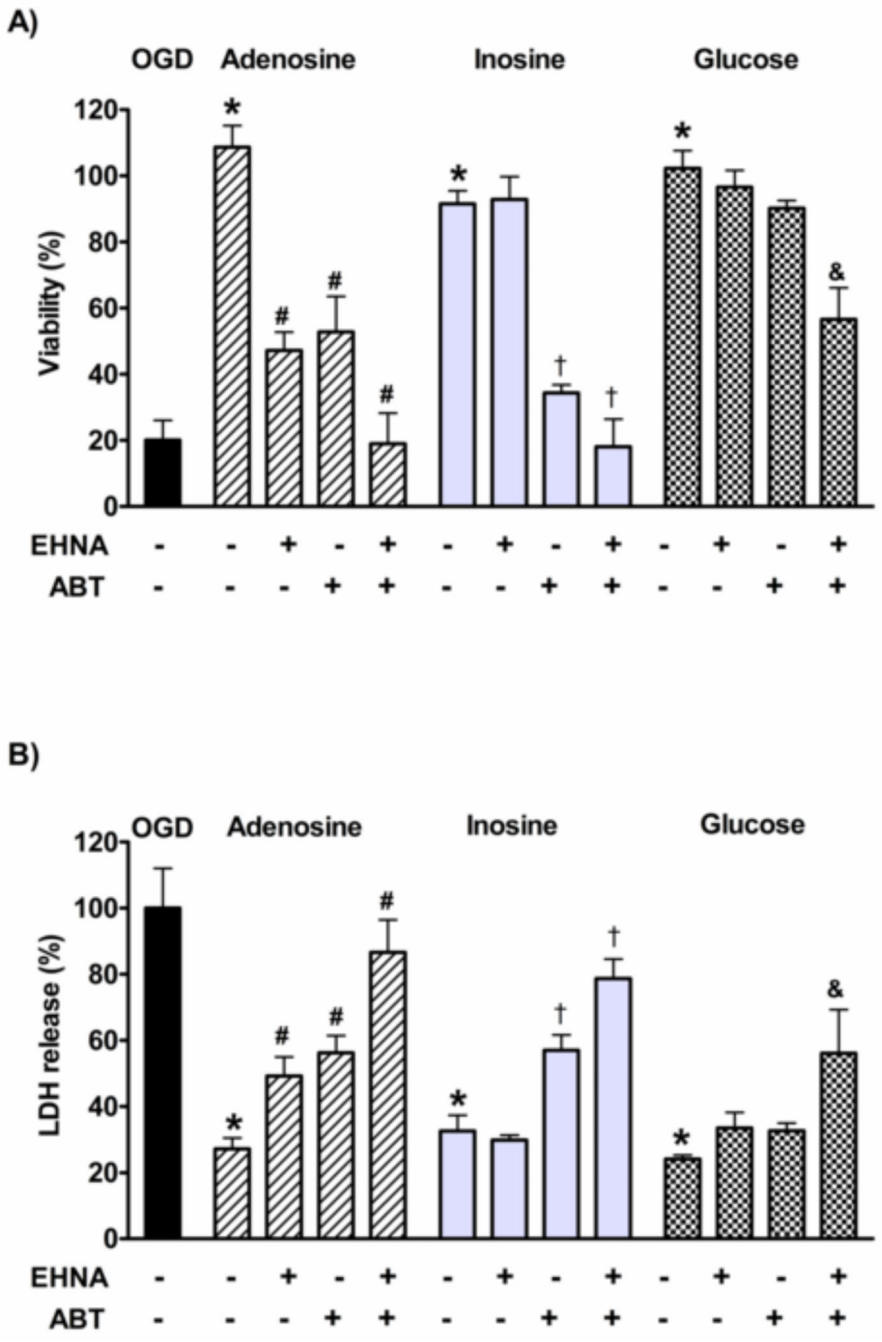

Figure 7. The role of adenosine deaminase (ADA) and adenosine kinase (AK) in the cytoprotective effects of adenosine, inosine and glucose in hypoxia-reoxygenation injury

LLC-PK1 cells pretreated with ADA inhibitor EHNA (10 μM) and/or AK inhibitor ABT702 (ABT, 30 μM) were subjected to 20-hour-long hypoxia in the absence (OGD) or presence of 300μM adenosine, inosine or glucose. Following the hypoxia, the cells were re-supplied with oxygen and glucose for 24 hours and the viability was evaluated by MTT assay and expressed as percent values of controls (A). LDH activity was measured in the supernatant (B), data are percent values of the activity measured in the supernatant of the OGD group.

(Mean ± SD values are shown. *p<0.05 compared to OGD, #p<0.05 compared to adenosine, †p<0.05 compared to inosine, &p<0.05 compared to glucose).

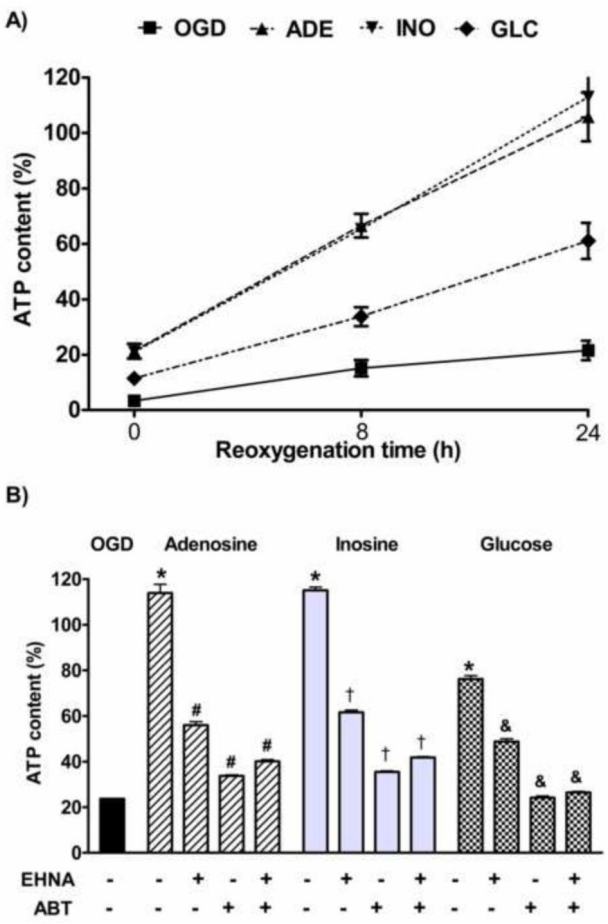

Figure 8. The posthypoxic ATP content of the cells after purine nucleoside supplementation and the effect of ADA and AK inhibition on the recovery

LLC-PK1 cells were subjected to 20 hour-long hypoxia in the absence (OGD) or presence of 300 μM adenosine (ADE), inosine (INO) or glucose (GLC), then re-supplemented with glucose and oxygen and incubated up to 24 hours. The ATP content was determined at the indicated reoxygenation time and expressed as percent values of control cells (A). After the hypoxia the cells were also treated with ADA inhibitor EHNA (10μM) and/or AK inhibitor ABT 702 (ABT, 30μM) and the ATP content was measured after 24 hours (B). (Data are shown as mean ± SD values. *p<0.05 compared to OGD, #p<0.05 compared to adenosine, †p<0.05 compared to inosine, &p<0.05 compared to glucose.)

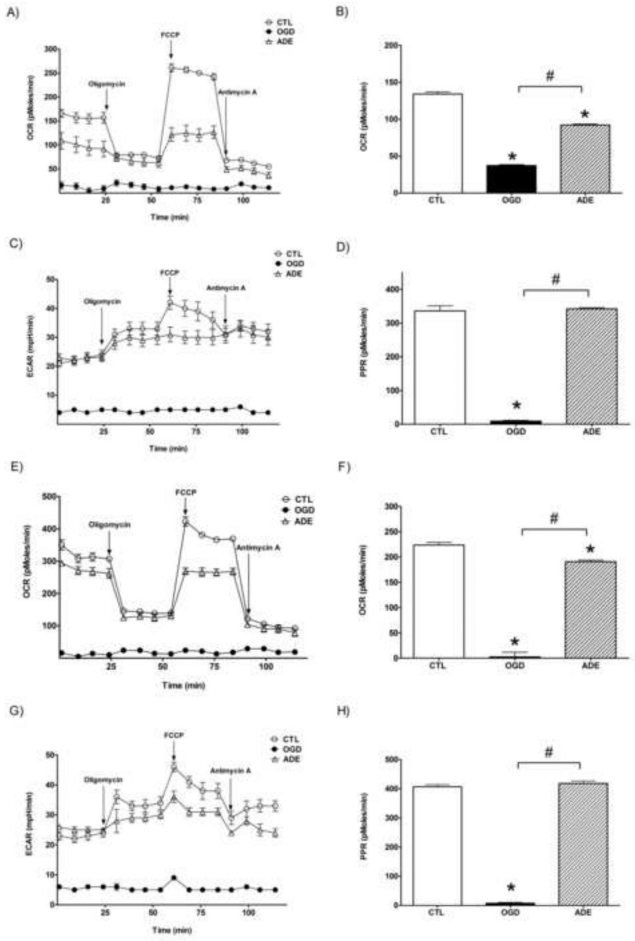

Figure 9. Seahorse metabolic analysis of LLC-PK1 cells subjected to hypoxia-reoxygenation injury

LLC-PK1 were subjected to hypoxia in the absence (OGD) or presence of 300 μM adenosine (ADE) for 20 hours and analyzed immediately (A-D) or re-supplemented with glucose and oxygen and incubated for 24 hours prior to the measurement (E-F). Oxygen consumption rate (OCR) and the extracellular acidification rate (ECAR) were determined prior to and after the addition of oligomycin, FCCP and antimycin A (A,C,E,F), as indicated on the figure. The basal respiration (B,F) as the difference between the OCR prior to oligomycin and after antimycin A and the respective proton production rates (PPR) are also shown (D,H). (Data are shown as mean ± SEM values. *$p<0.05$ compared to CTL, #$p<0.05$ compared to OGD)

Table 1

The LOPAC molecules showing the highest protective effect in the hypoxia screens

Hypoxia-reoxygenation injury was induced in LLC-PK1 cells and the LOPAC library was screened for protective effect in various set-ups. From each screen the ten highest-ranking cytoprotective compounds are shown with the respective activity in the other assays and the known biological function. (I.) In the pre-treatment screen (PRE) the compounds (50 μM) were applied prior to the OGD, (II.) in the post-treatment screen (POST) the cells received the compounds after the OGD. Adenosine pretreatment (30 μM) was combined (III.) with compounds pre-treatment (ADE PRE) and (IV.) with the application of the test compounds following the hypoxia (ADE POST). The shown cytoprotective effect represents the increase in viability compared to the OGD in PRE and POST screens or compared to the adenosine-treated cells subjected to OGD (ADE) in ADE PRE and ADE POST screens. (The viability values of CTL, OGD and ADE groups were 100%, 40% and 70%, respectively.)

Compound	Known biological activity	Cytoprotection (%)			
		PRE	POST	ADE PRE	ADE POST
I. Pre-treatment screen					
Adenosine	*endogenous neurotransmitter*	**46.0**	13.2	16.6	−0.8
Disulfiram	*aldehyde dehydrogenase inhibitor*	**34.5**	2.9	−9.2	0.8
2-Phenylaminoadenosine	*selective adenosine A2 receptor agonist*	**33.5**	1.9	−4.2	2.6
Tyrphostin AG 537	*tyrosine kinase inhibitor*	**32.6**	4.1	−14.4	7.1
Riluzole	*glutamate release inhibitor*	**30.4**	−1.1	−2.1	10.6
Tyrphostin 1	*tyrosine kinase inhibitor*	**30.3**	2.5	1.4	2.0
Zardaverine	*phosphodiesterase(PDE) inhibitor*	**28.3**	4.3	−13	−1.5
Triamcinolone	*glucocorticoid steroid*	**27.2**	3.3	1.1	1.5
Thapsigargin	*SERCA inhibitor*	**26.3**	3.0	−15.1	−3.1
Vinblastine sulfate	*inhibitor of microtubule assembly*	**23.3**	4.3	−25.2	−9.3
II. Post-treatment screen					
N-Acetyldopamine monohydrate	*dopamine analog possessing antitumor activity*	1.1	**15.4**	3.1	−3.5
Enoximone	*phosphodiesterase inhibitor*	4.2	**14.0**	−6.0	4.5
R(-)-N-Allylnorapomorphine HBr	*dopamine receptor anatagonist*	4.1	**13.5**	7.8	10.4
L-Aspartic acid	*amino acid, participant in gluconeogenesis*	1.0	**13.5**	8.3	24.8
Amperozide HCl	*serotonin receptor antagonist*	−6.4	**13.3**	−73.0	6.5
5α-Androstane-3α,17β-diol	*testosterone metabolite*	2.3	**13.2**	−2.6	−1.4
Adenosine	*endogenous neurotransmitter*	46.0	**13.2**	16.6	−0.8
4-DAMP methiodide	*M3 muscarinic acetylcholine receptor antagonist*	−4.6	**13.1**	−45.0	−1.6
Aminoguanidine HCl	*inhibitor of nitric oxide synthase (NOS)*	3.7	**13.0**	6.8	8.0
AEBSF	*serine protease inhibitor*	1.0	**12.9**	7.3	−1.3
III. Adenosine combined pre-treatment screen					
γ-D-Glutamylaminomethylsulfonic acid	*kainate/quisqualate glutamate receptor antagonist*	1.4	2.0	**27.0**	3.2
Hydrocortisone 21-hemisuccinate	*glucocorticoid steroid*	1.6	3.0	**25.1**	11.7
Tyrphostin AG 126	*TNF-α and NO synthesis inhibitor*	16.5	−0.9	**18.1**	3.6
4-Amino-1,8-naphthalimide	*poly(ADP-ribose) polymerase (PARP) inhibitor*	8.9	4.6	**16.9**	21.9
Adenosine	*endogenous neurotransmitter*	46.0	13.2	**16.6**	−0.8

Compound	Known biological activity	Cytoprotection (%)			
		PRE	POST	ADE PRE	ADE POST
Caffeic acid phenethyl ester	*NF- κ B inhibitor*	1.7	3.6	**12.4**	22.5
2-Methylthioadenosine diphosphate	*P2Y purine receptor agonist*	18.7	2.9	**11.1**	8.4
Bestatin hydrochloride	*aminopeptidase inhibitor*	5.1	2.6	**10.9**	−3.8
Thiocitrulline	*inhibitor of neuronal and endothelial NOS*	8.0	3.8	**9.3**	15.2
R(+)-6-Bromo-APB hydrobromide	*D1 dopamine receptor agonist*	0.5	3.8	**8.8**	14.3
IV. Adenosine combined post-treatment screen					
Arecaidine propargyl ester HBr	*M2 muscarinic acetylcholine receptor agonist*	−1.4	3.5	−16.1	**35.6**
L-Aspartic acid	*amino acid, participant in gluconeogenesis*	1.0	13.5	8.3	**24.8**
Centrophenoxine HCl	*cholinergic nootropic agent*	1.0	6.1	8.5	**24.0**
Caffeic acid phenethyl ester	*NF-kB inhibitor*	1.7	3.6	12.4	**22.5**
4-Amino-1,8-naphthalimide	*poly(ADP-ribose) polymerase (PARP) inhibitor*	8.9	4.6	16.9	**21.9**
KN-62	*Ca2+/calmodulin-dependent protein kinase inhibitor*	2.2	2.1	−40.2	**18.0**
Dipyridamole	*PDE and thromboxane synthase inhibitor*	2.2	8.1	3.4	**16.8**
Thiocitrulline	*inhibitor of neuronal and endothelial NOS*	8.0	3.8	9.3	**15.2**
R(+)-6-Bromo-APB hydrobromide	*D1 dopamine receptor agonist*	0.5	3.8	8.8	**14.3**
Hydrocortisone 21-hemisuccinate	*glucocorticoid steroid*	1.6	3.0	25.1	**11.7**

Abbreviations: SERCA: sarco/endoplasmic reticulum Ca^{2+}-ATPase, DAMP: 4-Diphenylacetoxy-N-methylpiperidine methiodide, AEBSF: 4-(2-Aminoethyl) benzenesulfonyl fluoride hydrochloride, R(+)-6-Bromo-APB hydrobromide: (+)-6-Chloro-7,8-dihydroxy-3-allyl-1-phenyl-2,3,4,5-tetrahydro-1H-3-benzazepine hydrobromide